THE ASTROPHYSICAL JOURNAL SUPPLEMENT SERIES, 72:163–189, 1990 January

AN ANALYSIS OF THE SHAPES OF ULTRAVIOLET EXTINCTION CURVES. III. AN ATLAS OF ULTRAVIOLET EXTINCTION CURVES

EDWARD L. FITZPATRICK[1]
Princeton University Observatory
AND
DERCK MASSA[1]
Applied Research Corporation
Received 1989 March 17; accepted 1989 July 12

ABSTRACT

In this paper, we assemble the basic data needed to produce UV extinction curves for a sample of 78 stars which have been analyzed in previous papers of this series. The data include spectral types, visual photometry, parameters used to produce fits to the UV extinction curves, distances to the program stars, and line-of-sight H I column densities (most of which are newly determined from low-dispersion *IUE* data).

We also include a detailed discussion of the observational and numerical techniques employed to obtain the results, so that the process can be reproduced easily.

The UV extinction curves and their analytic fits are displayed graphically. In this way, the reader can easily assess how well the fits obtained by the curve parameterization scheme represent the data, and the quality of the observations used to derive the fits.

Subject headings: interstellar: abundances — interstellar: matter — ultraviolet: spectra

I. INTRODUCTION

Since its launch in 1978, the *IUE* satellite (Boggess *et al.* 1981*a*, *b*) has provided a wealth of data on the wavelength dependence of interstellar extinction in the ultraviolet (UV). The low-dispersion mode of *IUE* covers the wavelength range ~1170–3200 Å at a resolution of ~6 Å and has been particularly valuable for extinction studies. In a recent series of papers (Massa and Fitzpatrick 1986; Fitzpatrick and Massa 1986, 1988, hereafter papers I and II), we sought first to understand the errors which affect *IUE* UV extinction measurements and then to codify the shapes of the extinction curves by an analytic representation, while keeping an eye toward physical interpretations. This has been an ongoing process, and, as a result, both the working sample of curves and the parameterization scheme used to describe them have evolved from those introduced by Massa and Fitzpatrick to the most recent ones employed in Paper II.

The main objective of this paper is to bring together all of our previous results and to present them in a uniform manner. These data are supplemented with additional basic information about the program stars, including the H I column densities and the distances to each star. The distances are useful for transforming quantities into mean line-of-sight densities which are useful for physical interpretations (see, e.g., Spitzer 1985). Another objective is to summarize the details of the analytical approach used to prepare and parameterize the curves so that additional curves can be analyzed in a format which is completely consistent with the results given here. In these respects, the present work differs somewhat in scope and intent from the recent compilation of *IUE* extinction curves published Aiello *et al.* (1988).

With the information presented here, individual extinction curves can be constructed easily and the quality of the fits assessed. It is hoped that by placing these data in an easily accessible form, they will be more useful to other investigators studying a variety of applications. They could, for example, be incorporated into depletion studies, as by Jenkins, Savage, and Spitzer (1986) and Joseph *et al.* (1986). They will also be useful for testing the predictions by different grain models, especially when used in conjunction with extinction or dust emission data at other wavelengths (see, for example, Jura 1980). In addition, they may also find applications in further investigations of the regional variability UV extinction curves and the errors that this variability can introduce into dereddened spectra.

Section II presents the basic equations and definitions used throughout the paper. In § III, we give our selection criteria for the program stars and list their observed properties. In § IV, we describe the details of how the curves are produced and fitted, and our results are presented in § V.

II. PRELIMINARIES

All of the UV extinction curves discussed here are pair method curves normalized by $E(B-V)$. To construct these curves, one first selects a lightly reddened comparison star or "flux standard" whose spectral features match those of a reddened program star as closely as possible. An extinction

[1]Guest observers with the *International Ultraviolet Explorer* satellite, which is sponsored and operated by the National Aeronautics and Space Administration, the Science Research Council of the United Kingdom, and the European Space Agency.

curve is then constructed by the relationship,

$$k(\lambda - V) \equiv \frac{E(\lambda - V)}{E(B-V)} = \frac{m(\lambda - V) - m(\lambda - V)_{\rm STD}}{(B-V) - (B-V)_{\rm STD}}, \quad (1)$$

where $m(\lambda - V)$ and $B-V$ are the UV and visual colors of the reddened program star, and $m(\lambda - V)_{\rm STD}$ and $(B-V)_{\rm STD}$ are the dereddened colors of the flux standard.

The scheme introduced in Paper II for parameterizing UV extinction curves is based upon the empirical result that the entire UV extinction curve can be represented accurately by a combination of three basic elements. Defining $x \equiv \lambda^{-1}$, these are (1) a linear "background" term, (2) a Lorentzian-like "Drude" profile, $D(x; \gamma, x_0)$, which represents the 2175 Å bump, and (3) a far-UV curvature term, $F(x)$. The complete parameterized function is given by

$$k(x - V) = c_1 + c_2 x + c_3 D(x; \gamma, x_0) + c_4 F(x), \quad (2)$$

where

$$D(x; \gamma, x_0) = \frac{x^2}{\left(x^2 - x_0^2\right)^2 + x^2\gamma^2}, \quad (3)$$

and

$$F(x) = \begin{cases} 0.5392(x-5.9)^2 + 0.05644(x-5.9)^3 \\ \qquad \text{for } x \geq 5.9\,\mu\text{m}^{-1}, \\ 0 \\ \qquad \text{for } x < 5.9\,\mu\text{m}^{-1}. \end{cases} \quad (4)$$

Fitting an extinction curve by equation (2) determines the values of six parameters, c_1, c_2, c_3, c_4, γ and x_0. As we shall see, equation (2) produces excellent fits to the observed curves throughout the entire UV. As a result, all of the information contained in an *IUE* UV extinction curve can be distilled into these six numbers.

Although not employed here, it should be pointed out that both Carnochan (1986) and ourselves (Paper II) have found that the slope and intercept of the linear term are not independent. In fact, they could be combined into a single term of the form, $c'(x - 3.00) + 2.04$. In this case, the two parameters c_1 and c_2 are replaced by a single parameter c', reducing the number of free parameters needed to fit the curves to 5.

The idea of fitting the bump region with a combination of a function linear in x and a Lorentzian was introduced by Savage (1975) and was carried out by Seaton (1979). In Paper I, we adopted a slight variation on the Lorentz profile which we refer to as the Drude profile. In fact, it is simply the full expression for the absorption cross section due to a forced-damped harmonic oscillator and reduces to a Lorentzian near resonance (see, Jackson 1962, p. 602). It was adopted because it produces slightly better fits to the data than the Lorentzian profile, and, more important, it is useful for interpreting the results in terms of simple semiclassical models for solids, such as the Drude model (see Bohren and Huffmann 1983).

In Paper II, we showed that $F(x)$ describes the far-UV curvature of all of the stars in our sample with remarkable accuracy. As a consequence, we were able to eliminate the need for separate quadratic and cubic terms (in x) to fit the far-UV extinction and to replace them with the single "universal" term, $F(x)$.

It should be pointed out that γ and x_0 are fundamentally different from the other parameters. The c's are directly dependent upon the choice of normalization. For example, if we were to change the $E(B-V)$ normalization given in equation (1) to the $A(V)$ normalization adopted by Cardelli, Clayton, and Mathis (1988), the c's would change accordingly. On the other hand, γ and x_0 would not. They are, in this sense, scale-free parameters.

III. THE SAMPLE

Our sample of reddened stars consists of two general groups which we refer to as "cluster stars" and "program stars." The cluster stars are the sample studied by Massa and Fitzpatrick (1986) in order to establish the accuracy of *IUE* extinction curve measurements. This group consists of 33 stars in the galactic clusters NGC 2244, NGC 3293, NGC 6231, Trumpler 14, and Cepheus OB 3. The program star sample refers to the 45 stars studied in Papers I and II. These stars sample a wide range of interstellar environments and represent some of the most unusual extinction observed by *IUE*. In addition, we include a group of 11 lightly reddened flux standards, all taken from the *IUE* spectral atlas (Wu *et al.* 1983).

We confined the stars in our sample to normal OB stars near the main sequence. The earliest type used is set by the availability of the lightly reddened flux standards needed to produce pair method extinction curves. Good spectral coverage is available up to O7 for stars near the main sequence. Very luminous stars are avoided because of a shortage of flux standards and because luminosity mismatch can produce large errors when stars more luminous than class III are employed (see the discussion in Massa, Savage, and Fitzpatrick 1983). We also confine our sample to stars B5 and earlier. However, later B stars could probably be included without a significant loss of accuracy. Savage *et al.* (1985) use *ANS* data to demonstrate that extinction curves derived from stars as late as B7 are relatively insensitive to small temperature mismatches. For later types, small temperature mismatches produce very strong effects on the far-UV. Although this limits the usefulness of the far-UV data derived from these stars, it may still be possible to obtain accurate measurements of the 2175 Å bump from much later stars.

Many of the program stars were selected because they sample unusual dust environments such as reflection nebula, dark clouds, and H II regions. The dust along these lines of sight produce some of the most extreme extinction curves obtained from *IUE* observations. As a result, the sample is biased toward extinction curves which appear abnormal when compared to a galactic mean curve such as Seaton's (1979). An investigation of a more unbiased sample is given by Massa (1987).

Basic properties of the program stars are listed in Table 1. Column (1) gives HD numbers, when available; column (2) lists either common names, BD or CPD numbers, or specific names for stars without HD, BD, or CPD numbers. These are "Oo" for Per OB 1 stars (Oosterhoff 1937), "Tr14" for

TABLE 1

OBSERVATIONAL DATA FOR PROGRAM STARS

HD	Other	Sp. Type	Ref.[a]	ℓ (°)	b (°)	V	B-V	U-B	Ref.[b]	Distance[c] (kpc)	log N(HI)	Ref.[d]
13338	...	B1 V	MCW	133.5	-3.3	9.03	0.25	-0.55	Hil	1.07	21.53	IUE
14250	Oo1586	B1 III	JM	134.8	-3.7	8.96	0.32	-0.54	JM	3.30	21.52	IUE
21483	...	B3 III	MCW	158.9	-21.3	7.03	0.35	-0.33	Hil	0.32	21.0:	IUE
34078	AE Aur	O9.5 V	W72	172.1	-2.3	5.97	0.23	-0.69	Rac	0.46	21.20	SVS
36982	LP Ori	B2 V	LA	209.1	-19.4	8.60	0.10	...	Pan	0.40	21.60	IUE
37022	θ^1 Ori C	O6p	MCW	209.0	-19.4	5.13	0.02	-0.95	Bla	0.40	21.60	IUE
37023	θ^1 Ori D	B0.5 Vp	Hof	209.0	-19.4	6.70	0.09	...	Bla	0.40	21.54	IUE
37061	NU Ori	B0.5 Vb	LA	208.9	-19.3	7.03	0.26	...	Pan	0.40	21.70	IUE
37367	...	B2 IV-V	Bla	179.0	-1.0	5.95	0.16	-0.51	Cra	0.26	21.52	IUE
37903	...	B1.5 V	Sha	206.9	-16.5	7.82	0.10	-0.62	Bla	0.82	21.28	IUE
38087	...	B3:	Sha	207.1	-16.3	8.30	0.13	-0.48	HHT	0.52	21.48	IUE
38131	...	B0.5 V	MCW	174.6	+3.2	8.19	0.21	-0.69	Hil	1.13	21.52	IUE
46056	...	O8 Vn	W71	206.3	-2.3	8.15	0.19	-0.74	Hil	2.06	21.18	SVS
46202	...	O9 V	W71	206.3	-2.0	8.17	0.17	-0.74	J55	1.59	21.20	IUE
48099	...	O7 V	W72	206.2	+0.8	6.38	-0.05	-0.95	Hil	1.28	21.20	SVS
73882	...	O8.5 V((n))	W73	260.2	+0.6	7.24	0.40	-0.55	Nic	0.85	21.11	IUE
91824	...	O7 V((f))	W72	285.7	+0.1	8.17	-0.05	-0.95	TGH	2.93	21.15	IUE
93028	...	O9 V	W72	287.6	-1.2	8.36	-0.06	-0.89	FMF	2.42	20.95	IUE
93222	...	O7 III((f))	W72	287.7	-1.0	8.08	0.08	-0.84	FMF	3.08	21.54	IUE
147701	...	B5 V	Gar	352.3	+16.8	8.35	0.57	-0.08	HC	0.25	21.60	Rho
147888	ρ Oph D	B3 V:	Ber	353.6	+17.7	6.74	0.32	-0.34	HC	0.29	21.60	Rho
147889	...	B2 V	Gar	352.9	+17.0	7.86	0.85	-0.16	HC	0.22	21.70	IUE
147933	ρ Oph AB	B2 IV+V	HGS	353.7	+17.7	4.63	0.22	-0.55	Nic	0.20	21.60	SVS
149757	ζ Oph	O9.5 V	MCW	6.3	+23.6	2.56	0.02	-0.86	J55	0.13	20.72	Boh
154445	...	B1 V	MCW	19.3	+23.0	5.63	0.16	-0.66	Cou	0.26	21.11	IUE
167771	...	O7 III:(n)((f))	W72	12.7	-1.1	6.54	0.12	-0.84	HJ	1.43	21.10	IUE
185418	...	B0.5 V	MCW	53.6	-2.2	7.45	0.22	-0.67	Hil	0.79	21.11	IUE
193322	...	O9 V:((n))	W72	78.1	+2.8	5.84	0.11	-0.77	HJ	0.59	21.08	BSD
197512	...	B1 V	Gue	87.9	+4.6	8.56	0.06	-0.69	Gue	1.13	21.26	IUE
199579	...	O6 V((f))	W73	85.7	-0.3	5.96	0.05	-0.85	Hil	0.92	21.08	BSD
203938	...	B0.5 IV	MCW	90.6	-2.2	7.08	0.46	-0.41	Hil	1.34	21.48	IUE
204827	...	B0 V	MCW	99.2	+5.5	7.95	0.81	-0.15	Hil	0.42	21.72	EBV
229196	...	O6 III(n)(f)	W73	78.8	+2.1	8.54	0.90	-0.15	Hil	1.18	21.77	EBV
239729	...	B0 V	W71	99.3	+3.7	8.35	0.36	-0.54	Sim	0.96	21.15	IUE
251204	...	B1: V:	Hil	187.0	+1.0	10.28	0.48	-0.55	Hil	1.29	21.57	EBV

TABLE 1—*Continued*

HD	Other	Sp. Type	Ref.[a]	ℓ (°)	b (°)	V	B-V	U-B	Ref.[b]	Distance[c] (kpc)	log N(HI)	Ref.[d]
252325	...	B0 IV	Hil	189.8	+0.4	10.79	0.57	-0.43	Hil	3.01	21.62	EBV
...	+56 524	B1 Vn	Sch	134.7	-3.7	9.75	0.34	-0.49	JM	1.31	21.4:	IUE
...	+57 513	B1 III	Hil	133.5	-3.1	9.50	0.29	-0.56	Hil	2.54	21.60	IUE
...	+59 562	O8 V	MCW	137.4	+1.0	9.73	0.47	-0.53	Hil	2.86	21.65	IUE
...	+60 594	O9 V	MCW	137.4	+2.1	9.30	0.36	-0.64	Hil	2.05	21.52	IUE
...	-59 2600	O6 V((f))	W73	287.6	-0.7	8.61	0.21	-0.78	FMM	2.47	21.48	SVS
...	H 36	O7.5 V(n)	W82	6.0	-1.2	10.30	0.57	-0.57	J67	1.40	21.95	IUE
...	Hilt 188	B1 V	Hil	131.1	-1.8	9.96	0.43	-0.40	Hil	1.29	21.48	IUE
...	Oo936	B1.5 V	Sch	134.6	-3.7	10.33	0.29	...	Wil	1.85	21.57	IUE
...	Tr14 No.20	O6 V	UV	287.4	-0.6	9.61	0.28	-0.73	FMM	3.55	21.48	IUE

[a]Spectral type references.—Ber, Bertiau 1958. Bla, Blaauw 1956. Gar, Garrison 1967. Gue, Guetter 1968. HGS, Hiltner, Garrison, and Schild 1969. Hil, Hiltner 1956. Hof, Hoffleit 1982. JM, Johnson and Morgan 1955. LA, Levato and Abt 1976. MCW, Morgan, Code, and Whitford 1956. Sch, Schild 1965. Sha, Sharpless 1952. UV, estimated equivalent spectral type derived by authors from low-dispersion *IUE* spectrum. W71, Walborn 1971. W72, Walborn 1972. W73, Walborn 1973. W82, Walborn 1982.

[b]Photometry references.— Bla, average from values tabulated by Blanco *et al.* 1968. Cou, Cousins 1964. Cra, Crawford 1963. FMF, Feinstein, Marraco, and Forte 1976. FMM, Feinstein, Marraco, and Muzzio 1973. Gue, Guetter 1975. HC, Hardie and Crawford 1961. Hil, Hiltner 1956. HHT, Hardie, Heiser, and Tolbert 1964. HJ, Hiltner and Johnson 1956. J55, Johnson 1955. J67, Johnson 1967. JM, Johnson and Morgan 1955. Nic, Nicolet 1978. Pan, Panek 1983. Rac, Racine 1968. Sim, Simonson 1968. TGH, Turner *et al.* 1980. Wil, Wildey 1964.

[c]Distances were computed using the absolute magnitude calibrations of Walborn 1972 for stars earlier than type B2 and Lesh 1968 for stars of type B2 and later. A distance of 400 pc was assumed for the four Orion nebula region stars, and we assume that the distance to Herschel 36 is the same as the distance to NGC 6530, 1.8 kpc, as determined by van Altena and Jones 1972.

[d]H I column density references.—Boh, Bohlin 1975. BSD, Bohlin, Savage, and Drake 1978. *EBV*, value derived assuming $N(\text{H I})/E(B-V) = 4.8\times10^{21}$. *IUE*, value derived by authors from low-dispersion *IUE* data (see § IV*b*). Rho, value for ρ Oph AB adopted. SVS, Shull and Van Steenberg 1985.

TABLE 2

OBSERVATIONAL DATA FOR CLUSTER STARS

Star	Cluster[a]	Sp. Type	Ref.[b]	V	B − V	U − B	Ref.[c]
HD 46106	NGC 2244	B0 V	MHN	7.92	0.15	-0.75	J&H
HD 259105	"	B1.5 V	MHN	9.37	0.19	-0.68	J&H
No. 11	"	B1 V	MHN	9.73	0.18	-0.71	J&H
No. 14	"	B2 V	MHN	10.32	0.23	-0.52	J&H
No. 23	"	B2.5 Vn	MHN	11.22	0.27	-0.44	J&H
HD 303067	NGC 3293	B0.5 V	TGH	9.55	0.03	-0.76	TGH
HD 303068	"	B1 V	TGH	9.76	0.02	-0.77	TGH
CPD -57 3507	"	B1 IV	TGH	9.27	-0.04	-0.83	TGH
CPD -57 3528	"	B2 V	TGH	10.66	0.05	-0.63	TGH
No. 65	"	(B1 V)	Pho	9.85	0.03	-0.75	TGH
No. 86	"	(B1 V)	Pho	10.74	0.11	-0.69	TGH
HD 326309	NGC 6231	...	...	10.02	0.24	...	Hou
HD 326330	"	B0.5 V	SNW	9.41	0.19	-0.67	Avg
HD 336332	"	B0.5 V	SNW	9.70	0.24	-0.63	Avg
HD 326364	"	B0 IV	Hou	9.62	0.36	-0.58	Avg
CPD -41 7711	"	B2: V:nn	GS	9.80	0.17	-0.61	Avg
CPD -41 7719	"	B1 V	SHS	9.47	0.13	-0.68	Avg
CPD -41 7724	"	B0.5 V	GS	9.50	0.14	-0.66	Avg
CPD -41 7727	"	B1 V	GS	9.44	0.15	-0.64	Avg
CPD -41 7730	"	B1 V	GS	9.29	0.17	-0.70	Avg
CPD -41 7736	"	B1 Vn	SNW	10.21	0.26	...	Avg
CPD -41 7743	"	B0.5 V	SNW	9.76	0.25	-0.61	Avg
CPD -41 7753	"	B1 V	SNW	9.83	0.25	-0.63	Avg
Br 1017	"	B2 IV-V	GS	10.63	0.23	-0.49	Avg
HD 216658	Cep OB3	B0.5 V	Gar	8.91	0.70	-0.28	Gar
HD 216898	"	O8.5 V	Gar	8.04	0.54	-0.48	Gar
HD 217061	"	B1 Vn	Gar	8.79	0.70	-0.25	Gar
HD 217086	"	O7n	Gar	7.66	0.64	-0.42	Gar
HD 217979	"	B2 V	Gar	8.59	0.35	-0.50	Gar
BD +61 2365	"	B1 V	Gar	9.20	0.52	-0.45	Gar
BD +62 2125	"	B1.5 V	Gar	8.95	0.65	-0.26	Gar
BD +62 2154	"	B1 V	Gar	9.33	0.51	-0.42	Gar
No. 6	Tr 14	(B0.5 V)	Pho	11.23	0.19	-0.68	FMM
No. 21	"	(B0 V)	Pho	10.88	0.34	-0.63	FMM
No. 27	"	(B1 V)	Pho	11.32	0.30	-0.56	FMM

[a] Distance estimates and galactic coordinates for the clusters are as follows: NGC 2244, $d = 1.6$ kpc (Heiser 1977), $l = 206\overset{\circ}{.}4$, $b = -2\overset{\circ}{.}0$. NGC 3293, $d = 2.5$ kpc (Turner *et al.* 1980), $l = 285\overset{\circ}{.}9$, $b = 0\overset{\circ}{.}1$. NGC 6231, $d = 1.6$ kpc (Shobbrook 1983), $l = 343\overset{\circ}{.}5$, $b = 1°2$. Tr 14, $d = 2.7$ kpc (Turner and Moffat 1980) $l = 287\overset{\circ}{.}4$, $b = -0\overset{\circ}{.}6$. Cep OB 3, $d = 0.72$ kpc (Crawford and Barnes 1970), $l = 108°–112°$, $b = 2°–4°$.

[b] Spectral type references.—Gar, Garrison 1970. GS, Garrison and Schild 1979. Hou, Houck 1956. MHN, Morgan *et al.* 1965. Pho, estimated from optical photometry by the authors. SHS, Schild, Hiltner, and Sanduleak 1969. SNW, Schild, Neugebauer, and Westphal 1971. TGH, Turner *et al.* 1980.

[c] Photometry references.—Avg, average from Garrison and Schild 1979, Schild, Hiltner, and Sanduleak 1969; Schild, Neugebauer, and Westphal 1971; and Bok, Bok, and Graham 1966. FMM, Feinstein, Marraco, and Muzzio 1973. Gar, Garrison 1970. Hou, Houck 1956. J&H, averages from Johnson 1962 and Heiser 1977. TGH, Turner *et al.* 1980.

TABLE 3

OBSERVATIONAL DATA FOR FLUX STANDARD STARS

HD	Other	Spectral Type	Reference[a]	V	$B-V$	$U-B$	Reference[b]	$E(B-V)$[c]
47839.....	15 Mon	O7 V((f))	W72	4.65	−0.25	−1.06	J55	0.07
38666.....	μ Col	O9.5 V	W73	5.17	−0.28	−1.06	Nic	0.02
36512.....	ν Ori	B0 V	JM	4.62	−0.26	−1.07	Nic	0.04
55857.....	...	B0.5 V	HGS	6.11	−0.26	...	CS	0.02
31726.....	...	B1 V	MCW	6.15	−0.21	...	Nic	0.05
62747.....	...	B1.5 III	HGS	5.62	−0.19	...	Nic	0.06
64802.....	...	B2 V	HGS	5.49	−0.19	−0.73	Nic	0.05
61831.....	...	B2.5 V	HGS	4.84	−0.20	−0.64	CS	0.02
32630.....	η Aur	B3 V	JM	3.17	−0.18	−0.67	Nic	0.02
79447.....	...	B3 III	HGS	3.97	−0.18	−0.67	Nic	0.02
34759.....	ρ Aur	B5 V	JM	5.23	−0.15	−0.57	Nic	0.01

[a] Spectral type references.—HGS, Hiltner, Garrison, and Schild 1969. JM, Johnson and Morgan 1953. MCW, Morgan, Code, and Whitford 1956. W72, Walborn 1972. W73, Walborn 1973.

[b] Photometry references.—CS, Cousins and Stoy 1962. J55, Johnson 1955. Nic, Nicolet 1978.

[c] $E(B-V)$ derived using intrinsic colors of FitzGerald 1970.

Trumpler 14 stars (Feinstein, Marraco, and Muzzio 1973), "Hilt" for numbers assigned by Hiltner (1956), and "H 36" for Herschel 36 in NGC 6531 (see Hecht *et al.* 1983). Galactic coordinates are listed in columns (3) and (4). Columns (5) and (6) give the adopted spectral types and references, while columns (7)–(10) list photometry and its references. Distances, in kiloparsecs, are given in column (11). These are from spectroscopic parallax, using the absolute magnitudes from the sources listed in the footnotes and assuming $A(V)/E(B-V)=3.1$, unless noted otherwise. Neutral hydrogen column densities and their sources are listed in columns (12) and (13) (see § IV).

Table 2 lists the spectroscopic and photometric data for the cluster sample. The numbering systems for stars without standard names are from the following sources: NGC 2244, Johnson (1962); NGC 3293, Turner *et al.* (1980); NGC 6231, Braes (1967); Trumpler 14, Feinstein, Marraco, and Muzzio (1973). Galactic coordinates and distance estimates (and their references) for the clusters are given in the footnotes to the table.

Table 3 gives similar data for the stars used as flux standards, along with their adopted color excesses.

IV. ANALYSIS

a) Preparation of the Spectra

Table 4 lists the image numbers of the *IUE* spectra used for the program stars in Papers I and II. Similar information can be found in Massa and Fitzpatrick (1986, and references therein) for the cluster stars and in the *IUE* spectral atlas for the flux standards. Note that only LWR images are used for the long-wavelength (1950–3200 Å) spectra.

The spectra were acquired by a number of investigators, for a wide range of purposes, over a period between approximately 1979.0 through 1984.0. During this time, several changes occurred in the standard data processing techniques employed by Goddard and VILSPA. The SWP spectra processed prior to 1979 July 7 (SWP image numbers less than ~5700) are affected by an error in the intensity transfer function. Our spectra processed before this data were corrected with the Gaussian correction algorithm given by Holm and Schiffer (1980). All spectra processed after 1980 November 3 (SWP numbers greater than ~10,500 and LWR numbers greater than ~9200) were reduced with improved software which employs a narrower extraction slit. This extraction roughly doubles the number of data points in the spectra and increases the effective resolution by a small amount. Our sample contains spectra processed by both systems. In some cases, the spectra employed in the reddened star–flux standard pair are processed by different systems. However, this has a negligible effect on our results since all of the data are on the same absolute calibration system (Bohlin and Holm 1980), and we ultimately bin the extinction curves to a much lower resolution than either of the original formats.

The sensitivities of the *IUE* cameras, particularly the LWR, have degraded slowly since launch. This degradation is wavelength dependent and has been discussed by Bohlin and Grillmair (1988). Recent spectra show systematically lower flux levels than those obtained, say, 10 yrs ago, even when processed and calibrated identically. This can effect extinction curves if there is a large difference between the dates when the reddened star and its flux standard were observed. When this project was begun, no detailed studies of the degradation had been published and no correction algorithms were available. Luckily, all but one of the flux standards were observed between 1980.0 and 1981.5, near the middle of the time span of the reddened star observations. Therefore, the difference in epochs between the observations of the reddened stars and flux standards rarely exceeds 3 yr. Consequently, the influence of detector degradation on the extinction curves displayed in the atlas should be small. Naturally, the effects of detector degradation should be included in future analyses.

For each program star, the final UV spectrum used to derive its extinction curve was formed by combining multiple exposures (if available) from each of the two *IUE* cameras

TABLE 4

IUE DATA FOR PROGRAM STARS

Program Star	SWP Camera		LWR Camera	
	Image No.	Aperture	Image No.	Aperture
13338	15676	L+S	12098	L+S
14250	16405, 16406	L, L	12656, 12657	L, L
21483	15285	L	11799	L
34078	15683	L+S	12643, 12644	L+S, L+S
36982	13732	L+S	10367	L+S
37022	4280	L+S	1349, 1350, 1351	S, L+S, L+S
37023	4281	L+S	1352, 3782	L, S
37061	6954	L+S	5970	L+S
37367	15082	L+S	11610	L+S
37903	8057	L+S	7025	L+S
38087	9803, 14569	L+S, L+S	9276, 11159	L+S, L+S
"	16409	L+S	12660, 12661	L+S, L+S
38131	15679, 15680	L+S, L+S	12101, 12102	L+S, L+S
46056	6913	L	5875	L
46202	6911	L	5873	L
48099	4133, 16434	L+S, L	3664, 12684	L+S, L
73882	13979, 13980	L+S, L	10627, 10628	L+S, L
91824	21528	L	16997	L
93028	11244	L	9866	L
93222	11135	L	9805	L
147701	13443	L	10105	L+S
147888	17486	L	13772	L+S
147889	4338	L+S	2482, 3831	S, L+S
147933	6587, 6588, 6589	L, L, L	5639, 5640	L, L
149757	18252	L	14381	L
154445	11140	L	9769	L+S
167771	17487	L	13773	L+S
185418	17469	L	13755, 13756	L, L
193322	5638	L	4888	L
197512	14523, 14588	L+S, L+S	11094, 11184	L+S, L+S
199579	9429	L	8169, 8535	L, L+S
203938	17471	L	13758	L
204827	14530	L	9761, 11104, 11107	L+S, L, L
229196	14009	L	10662, 11613	L+S, L
239729	13451	L	10114	L+S
251204	15081	L	11608, 11609	L, L+S
252325	15083	L+S	11611	L+S
+56 524	20330	L	16252, 16253	L, L
+57 513	15674	L	12096	L+S
+59 562	9925	L	8636	L+S
+60 594	9921	L	8632	L+S
-59 2600	11137	L	9806, 9842	L, L
H 36	2808, 4221, 4222	S, L, L	2501, 3732, 3733	S, L, L
Hilt 188	7096	L	6032, 6033	L, L
Oo936	17531	L	13811	L
Tr 14 #20	21510	L	16992	L

[a]The quantity $E(B-V)/d$ is given in units of mag kpc^{-1}.

[b]Comparison star used for constructing HD 37903 and HD 147933 curves is an average of HD 31726 (B1 V) and HD 64802 (B2 V).

and then splicing these together to produce a single spectrum covering the entire *IUE* wavelength range. Because of the limited dynamic range of *IUE*, several exposures were frequently needed to obtain a single well-exposed spectrum over the wavelength range of a camera. The individual exposures were resampled onto a uniform wavelength grid at 1 Å intervals, weighted by their net intensity levels, and averaged. Small aperture (3″) spectra were scaled to the flux levels defined by the large aperture (10″×20″) spectra and were weighted appropriately. All saturated data points and points affected by detector reseaux, cosmic-ray "hits," microphonics noise in the LWR, and "hot pixels" were eliminated. If no "good" data are available in a particular wavelength range, a gap appears in the reduced spectrum and in the extinction curve derived from it. Finally, the SWP and LWR spectra were combined by averaging them over the region 1925–1970 Å. In retrospect, this averaging process is no longer recommended. Rather, it is more informative simply to join the data at a particular wavelength, such as 1950 Å. In this way, photometric errors which produce shifts between the zero points of the two cameras are more apparent, and their impact is easier to evaluate. The final spectra span the wavelength range 1170–3200 Å.

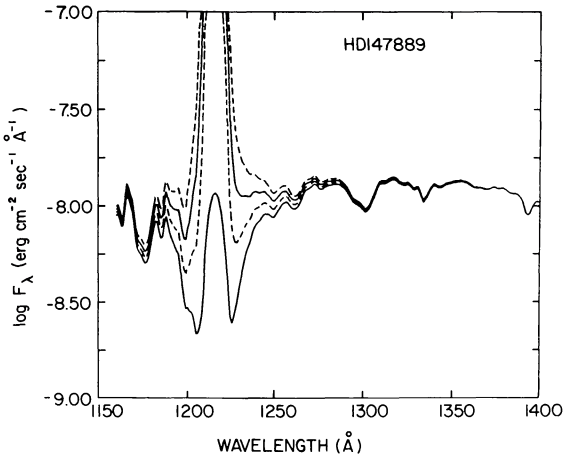

FIG. 1.—Example of the plots used to determine the neutral hydrogen column density, N(H I), toward the program stars. Results for HD 147889: lower solid curve is the raw, "uncorrected" spectrum, and upper solid curve gives the raw spectrum corrected for the adopted column density (2.5×10^{21} cm^{-2}). The two dashed curves result from correcting the raw spectrum by ±50% of the adopted column density. The central reversal in the spectrum is due to geocoronal Lyα emission.

b) *Correction for* Lyα *Absorption*

Neutral hydrogen absorption affects the spectra of heavily reddened stars throughout the range 1215±50 Å. It is desirable to correct the spectra for its effects in order to extend the amount of usable data and to estimate the neutral hydrogen column densities, N(H I), along the line of sight. The column densities are useful for determining mean gas-to-dust ratios toward the program stars. Several of the program stars have N(H I) measurements available in the literature. In these cases, we adopted the published N(H I) values. The spectra were corrected for the H I absorption by dividing them with a convolution of exp[$-N$(H I)$\phi(\lambda)$] and a 6 Å Gaussian. The Gaussian represents the *IUE* low-dispersion slit function, and $\phi(\lambda)$ is the absorption profile of H I given by Bohlin (1975):

$$\phi(\lambda)=\frac{4.26\times10^{-20}}{(\lambda-1215.67)^2+6.04\times10^{-10}}. \quad (5)$$

Most of the program stars do not have published N(H I) measurements. For these stars, we had to derive the column densities ourselves from the low-dispersion data. This was done by the usual method of convolving exp[$-N$(H I)$\phi(\lambda)$] with the *IUE* slit function for several values of N(H I) and dividing the spectra by a sequence of these functions. Once a spectrum assumes the appearance of one unaffected by Lyα absorption, that value of N(H I) is adopted (see, Bohlin 1975). Because of the order in which the convolutions are applied, this approach is not strictly valid. Nevertheless, the overall agreement between our results and those obtained from high resolution (discussed below) gives us confidence in our procedure.

An additional complication arises because the *IUE* platinum-neon wavelength comparison lamp lacks lines shortward of 1300 Å. As a result, wavelength calibration of the spectra is very poor in the neighborhood of Lyα, and it was necessary to shift them in wavelength in order to make the central position of the Lyα absorption align with 1215.67 Å. The center of the interstellar absorption was determined from the mean of the two half-intensity wavelengths on either side of the absorption (or geocoronal emission when present). The computed shifts were typically from −2 to −3 Å; i.e., the center of the absorption occurs near 1213 Å on the *IUE* scale.

To establish the appearance of spectra which are unaffected by Lyα absorption, we corrected several lightly reddened stars by values of N(H I) obtained from the literature. These corrected spectra were used as a grid against which the corrected fluxes of the program stars could be compared. Once a value of N(H I) was found which seems to eliminate the interstellar absorption, a plot was produced of the spectrum corrected by this value and by column densities ±50% of this value in order to assess the overall fit. Figure 1 gives one such plot for HD 147889. Finally, the region 1200–1230 Å was deleted from the spectra because of its very low signal and contamination by geocoronal emission.

In order to determine the accuracy of the low-dispersion N(H I) measurements, we also analyzed the low-dispersion spectra of heavily reddened stars whose N(H I) values are known from high-dispersion studies. Comparing the two sets of numbers enabled us to estimate the errors affecting the low-dispersion measurements. In no case was the disagreement greater than 40%, and typical differences were 20% or less. Since 25% is normally quoted as the absolute accuracy of the high-dispersion measurements (e.g., Shull and Van Steenberg 1985), our results suggest that column densities derived from the low-dispersion data have comparable accuracy.

Because we did not reanalyze the cluster star spectra from Massa and Fitzpatrick (1986), they were not corrected for Lyα absorption. Instead, a larger portion of the spectrum centered at 1215 Å was deleted. Specifically, the entire region from 1180–1250 Å was eliminated from these spectra.

TABLE 5

EXTINCTION CURVE DATA FOR PROGRAM STARS

Program Star	Flux Std	E(B − V)	$\frac{E(B-V)^a}{d}$	Curve Coefficients					
				λ_0^{-1}	γ	c_1	c_2	c_3	c_4
13338	31726	0.51	0.48	4.593	0.939	-0.032	0.794	3.977	0.377
14250	62747	0.57	0.17	4.570	0.950	-0.235	0.795	4.129	0.396
21483	79447	0.55	1.71	4.631	1.011	-0.278	0.730	2.367	0.658
34078	μ Col	0.53	1.14	4.589	1.087	0.473	0.571	4.151	0.520
36982	64802	0.34	0.85	4.575	0.873	1.101	0.050	2.638	0.311
37022	15 Mon	0.34	0.85	4.635	0.846	1.251	0.033	1.331	0.186
37023	55857	0.37	0.93	4.594	0.878	1.883	-0.083	1.215	0.153
37061	55857	0.54	1.35	4.581	1.074	1.309	0.109	2.041	0.044
37367	64802	0.40	1.52	4.601	0.901	0.708	0.555	3.985	0.260
37903	B 1.5[b]	0.35	0.38	4.615	1.045	0.965	0.384	3.300	0.440
38087	η Aur	0.33	0.64	4.563	1.026	1.137	0.230	4.508	0.311
38131	55857	0.49	0.43	4.607	0.955	-0.174	0.755	3.707	0.332
46056	15 Mon	0.51	0.25	4.611	0.932	-0.527	0.857	3.032	0.541
46202	μ Col	0.47	0.30	4.599	0.842	-0.348	0.864	2.542	0.515
48099	15 Mon	0.27	0.21	4.575	0.831	-0.856	0.874	2.979	0.339
73882	15 Mon	0.72	0.84	4.576	1.192	-0.412	0.788	3.341	0.540
91824	15 Mon	0.27	0.09	4.604	0.917	0.195	0.633	2.894	0.473
93028	μ Col	0.24	0.10	4.637	0.839	-0.757	0.811	1.557	0.166
93222	15 Mon	0.40	0.13	4.577	0.804	-0.053	0.626	1.697	0.236
147701	ρ Aur	0.73	2.91	4.615	1.135	1.290	0.329	3.581	0.888
147888	η Aur	0.52	2.61	4.587	1.022	1.611	0.133	3.823	0.339
147889	64802	1.09	5.02	4.617	1.082	1.449	0.151	4.473	0.709
147933	B 1.5[b]	0.47	2.36	4.593	0.969	1.642	0.139	3.349	0.349
149757	μ Col	0.32	2.46	4.595	1.383	-0.802	0.900	5.842	0.563
154445	31726	0.42	1.65	4.568	1.058	1.098	0.309	5.034	0.503
167771	15 Mon	0.44	0.31	4.561	0.974	-0.139	0.574	3.449	0.453
185418	55857	0.50	0.63	4.579	0.927	1.266	0.362	3.941	0.381
193322	μ Col	0.41	0.69	4.613	0.856	-0.617	0.879	2.264	0.115
197512	31726	0.32	0.28	4.585	1.006	-1.043	1.021	4.659	0.438
199579	15 Mon	0.37	0.40	4.606	0.997	-0.725	0.898	2.923	0.453
203938	55857	0.74	0.55	4.589	1.016	0.087	0.747	3.647	0.306
204827	υ Ori	1.11	2.65	4.623	1.077	-1.521	1.219	3.201	0.899
229196	15 Mon	1.22	1.03	4.581	0.990	-0.179	0.728	3.407	0.233
239729	υ Ori	0.66	0.69	4.605	1.075	0.076	0.728	3.391	0.685
251204	υ Ori	0.78	0.60	4.594	0.893	-0.671	0.861	2.862	0.383
252325	υ Ori	0.87	0.29	4.617	0.914	1.048	0.387	2.881	0.484
+56 524	31726	0.60	0.46	4.577	1.023	-0.690	0.917	4.027	0.496
+57 513	62747	0.54	0.21	4.589	0.909	-0.920	0.920	3.332	0.373
+59 562	15 Mon	0.79	0.28	4.595	0.907	-0.322	0.755	2.973	0.352
+60 594	μ Col	0.66	0.32	4.594	0.932	-0.548	0.819	3.457	0.411
-59 2600	15 Mon	0.53	0.21	4.594	0.950	0.087	0.601	2.448	0.179
H 36	15 Mon	0.89	0.63	4.620	0.886	1.680	0.055	1.998	0.312
Hilt 188	62747	0.68	0.53	4.603	0.934	-1.064	0.989	3.316	0.469
Oo936	31726	0.55	0.30	4.584	0.921	-0.411	0.902	3.638	0.531
Tr14 No.20	15 Mon	0.60	0.17	4.581	0.890	-0.180	0.729	2.287	0.383
LMC Average		...	...	4.608	0.994	-0.687	0.891	2.550	0.504
30 Dor Average		...	...	4.606	0.894	-2.186	1.388	1.488	0.425
Seaton Curve		...	...	4.595	1.051	-0.384	0.739	3.961	0.265

TABLE 6

EXTINCTION CURVE DATA FOR CLUSTER STARS

Star	Flux Std	E(B−V)	Curve Coefficients					
			λ_0^{-1}	γ	c_1	c_2	c_3	c_4
HD 46106	υ Ori	0.45	4.586	0.875	0.697	0.591	3.129	0.485
HD 259105	31726	0.45	4.598	0.855	0.165	0.595	2.927	0.467
NGC2244 No.11	31726	0.44	4.597	0.860	-0.007	0.645	2.932	0.464
NGC2244 No.14	64802	0.47	4.617	0.859	0.032	0.667	2.804	0.365
NGC2244 No.23	61831	0.49	4.575	0.927	-0.585	0.745	3.605	0.354
HD 303067	55857	0.31	4.616	1.094	0.033	0.733	3.192	0.147
HD 303068	31726	0.28	4.604	0.975	0.430	0.556	2.870	0.385
CPD -57 3507	31726	0.22	4.616	0.949	0.131	0.602	3.344	0.446
CPD -57 3528	64802	0.29	4.607	0.953	-0.368	0.756	2.707	0.404
NGC3293 No.65	31726	0.29	4.596	0.954	-0.425	0.835	2.924	0.526
NGC3293 No.86	31726	0.37	4.589	0.931	-0.062	0.751	3.119	0.515
HD 326309	31726	0.50	4.584	0.955	-0.080	0.719	3.515	0.477
HD 326330	55857	0.47	4.619	0.992	0.365	0.594	3.370	0.396
HD 336332	55857	0.52	4.577	0.976	0.193	0.653	3.482	0.304
HD 326364	υ Ori	0.65	4.601	1.034	0.117	0.634	3.772	0.420
CPD -41 7711	31726	0.43	4.604	0.987	-0.655	0.899	3.549	0.298
CPD -41 7719	31726	0.39	4.593	0.913	-0.087	0.729	3.393	0.522
CPD -41 7724	55857	0.42	4.589	0.919	0.396	0.684	3.081	0.375
CPD -41 7727	31726	0.43	4.605	0.942	0.013	0.712	3.134	0.385
CPD -41 7730	31726	0.43	4.593	0.922	-0.078	0.800	3.509	0.464
CPD -41 7736	31726	0.52	4.583	0.998	-0.214	0.743	3.529	0.402
CPD -41 7743	υ Ori	0.55	4.591	1.019	0.523	0.570	3.918	0.400
CPD -41 7753	55857	0.53	4.618	0.900	0.328	0.589	2.844	0.212
Br 1017	64802	0.47	4.592	0.952	-0.317	0.721	3.277	0.417
HD 216658	55857	0.98	4.600	1.042	0.321	0.568	3.859	0.426
HD 216898	μ Col	0.85	4.600	0.960	0.261	0.567	3.601	0.333
HD 217061	31726	0.96	4.597	0.986	0.072	0.638	3.527	0.588
HD 217086	15 Mon	0.96	4.598	1.006	0.496	0.484	3.968	0.399
HD 217979	31726	0.61	4.603	0.937	-0.305	0.781	3.117	0.580
BD +61 2365	31726	0.78	4.591	0.943	0.606	0.440	4.084	0.392
BD +62 2125	31726	0.91	4.593	0.986	-0.076	0.752	3.361	0.426
BD +62 2154	31726	0.77	4.598	0.984	0.433	0.544	3.721	0.457
Tr14 No.6	55857	0.47	4.585	0.943	0.485	0.465	2.518	0.383
Tr14 No.21	μ Col	0.64	4.578	0.978	-0.004	0.588	2.668	0.329
Tr14 No.27	31726	0.56	4.589	0.934	0.086	0.589	2.674	0.373

c) *Construction of the Extinction Curves*

To produce pair method curves, one must first have a suitable set of unreddened standard stars. All of the comparison stars have color excesses ≤ 0.07 mag. They were dereddened to the $(B-V)_0$ value appropriate for their spectral type (according to FitzGerald 1970) by applying Seaton's (1979) UV extinction curve. Massa (1987) shows that corrections for $E(B-V) \leq 0.10$ mag with a mean curve produce errors less than the photometric errors expected from *IUE* data. Because Lyα absorption is so small in these stars, they were not corrected for its effects.

Next, the reddened program stars were matched with flux standards on the basis of their UV spectra. The identification of features useful in matching B stars near the main sequence is given by Massa, Savage, and Fitzpatrick (1983) and Massa, Savage, and Cassinelli (1984). Once the star pair is selected, their spectra are divided to produce a flux ratio. This ratio is then binned to reduce noise and the number of data points which must be handled by the fitting routine. The binning is done on a λ^{-1} scale, with 0.05 μm^{-1} bins spanning the range $3.3\ \mu m^{-1} < \lambda^{-1} < 8.7\ \mu m^{-1}$. The binned values of the flux ratio are simply the mean value of the data points within each bin. Should a program star lack data within a given bin, then the value of the binned ratio is 0. Note that the binning must be done before converting the flux ratios to magnitudes

TABLE 7

EMPIRICAL UNCERTAINTIES IN EXTINCTION CURVE COEFFICIENTS

T Coefficient	σ_0
λ_0^{-1}	0.0056
γ	0.020
c_1	0.16
c_2	0.037
c_3	0.13
c_4	0.037

NOTES.—The quantity σ_0 gives the uncertainty in each of the respective coefficients for an extinction curve with $E(B-V)=1.0$. The values of the uncertainties for other values of $E(B-V)$ are given by $\sigma = \sigma_0 / E(B-V)$.

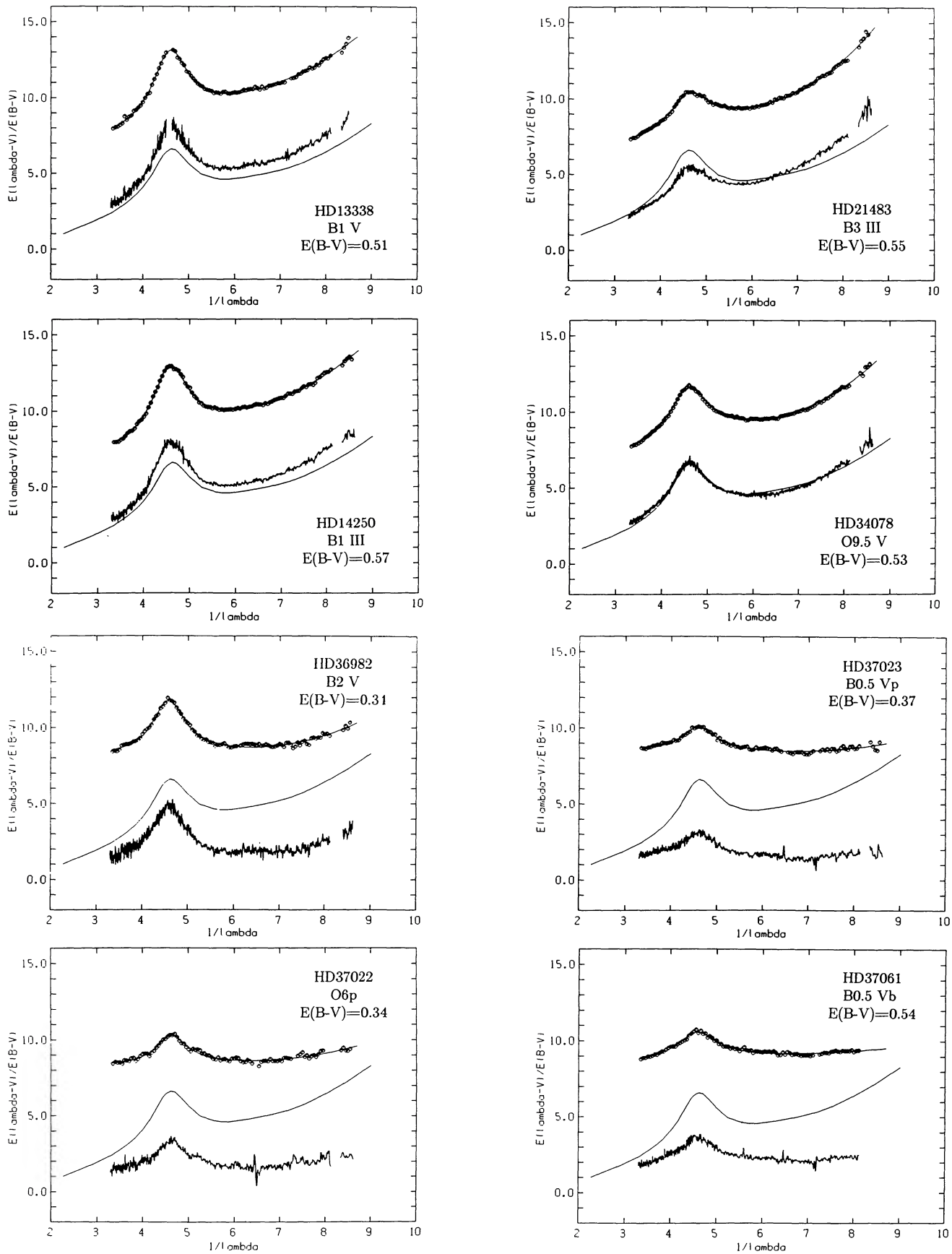

FIG. 2.—Extinction curves for the program stars. The lower portion of each plot shows the unbinned data, along with Seaton's (1979) mean galactic curve. Displaced by five units (typically) above these curves are the binned data, represented as discrete points, and the analytic fits to these data, given by solid lines. The star's name, spectral type, and color excess are included on each plot.

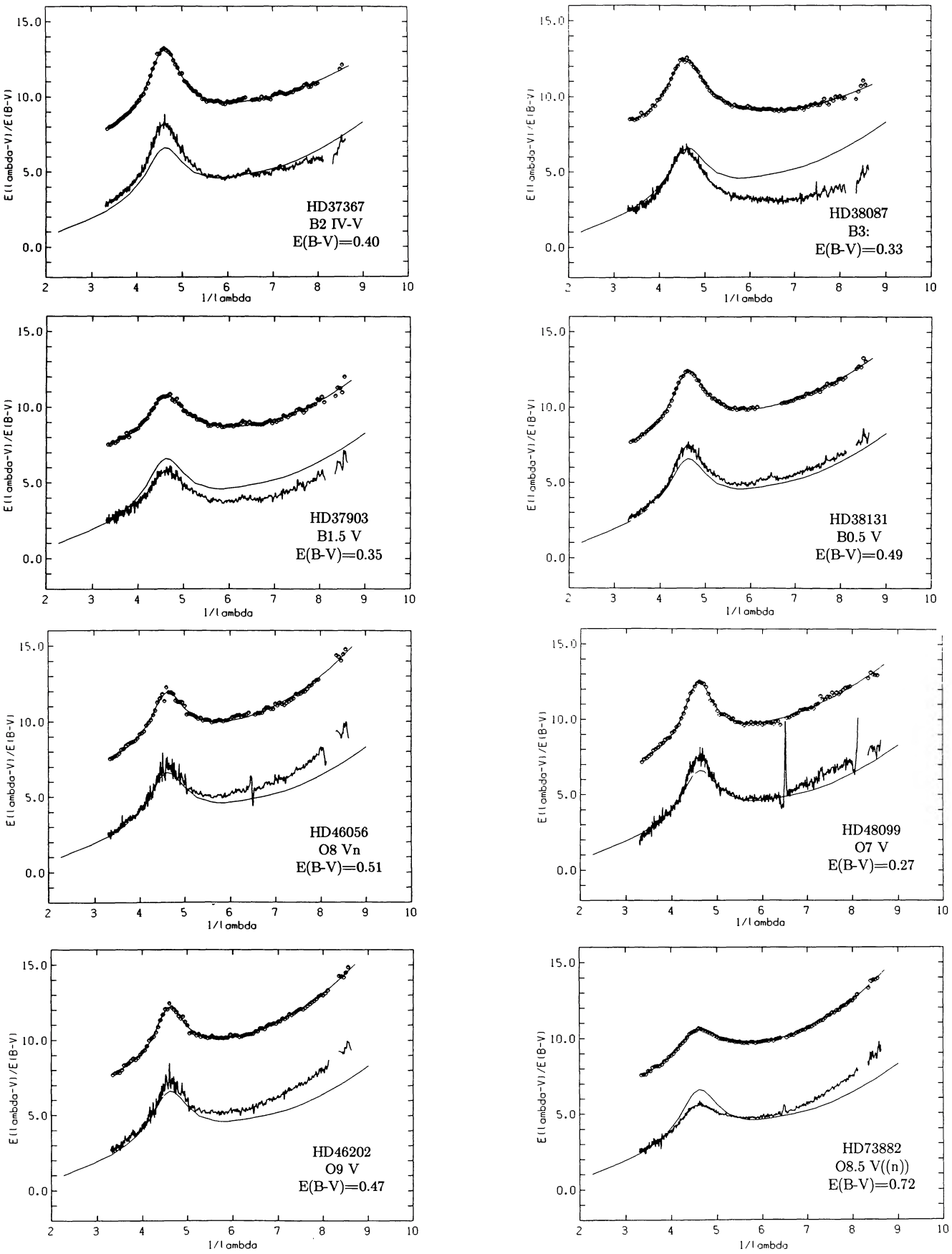

FIG. 2—*Continued*

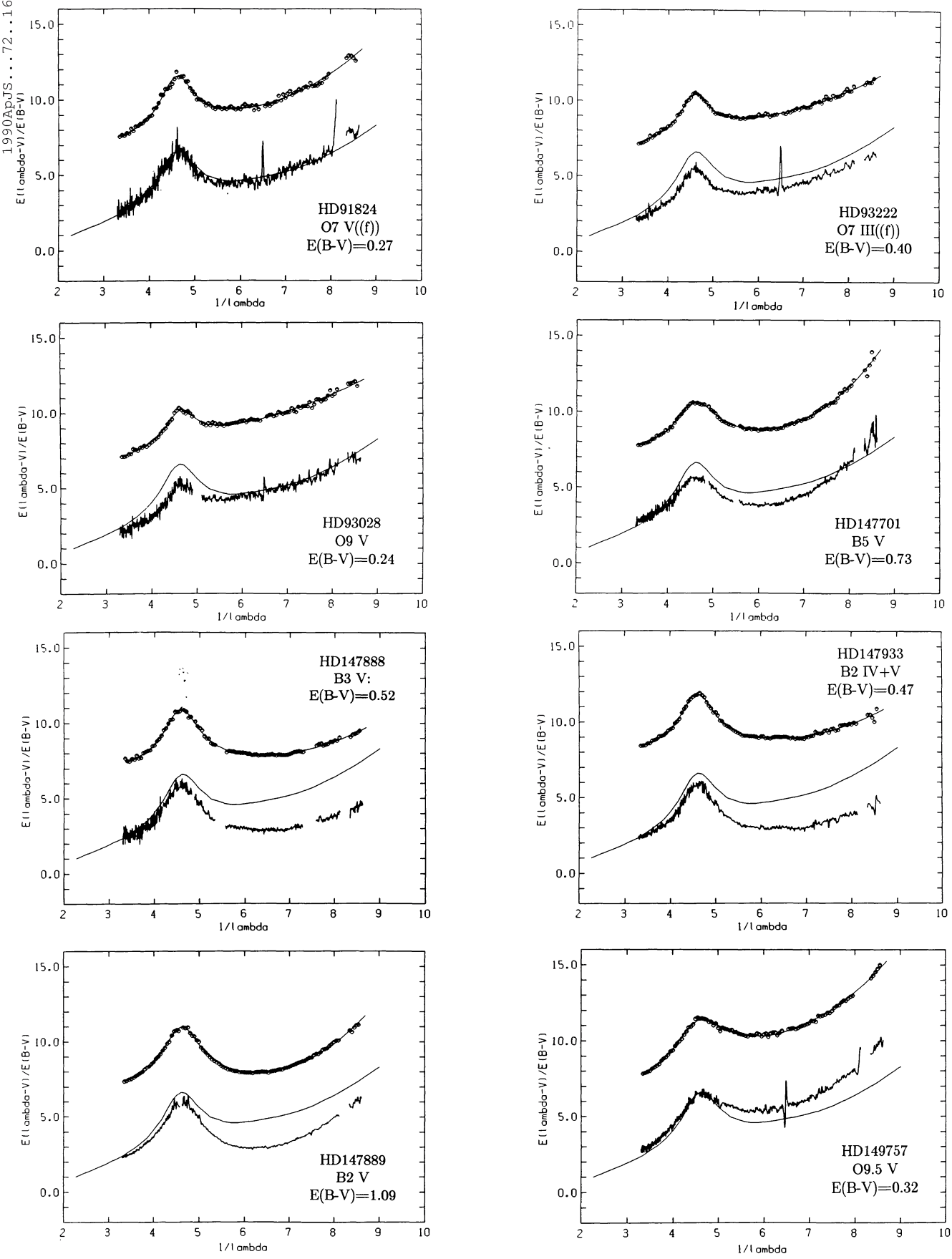

FIG. 2—*Continued*

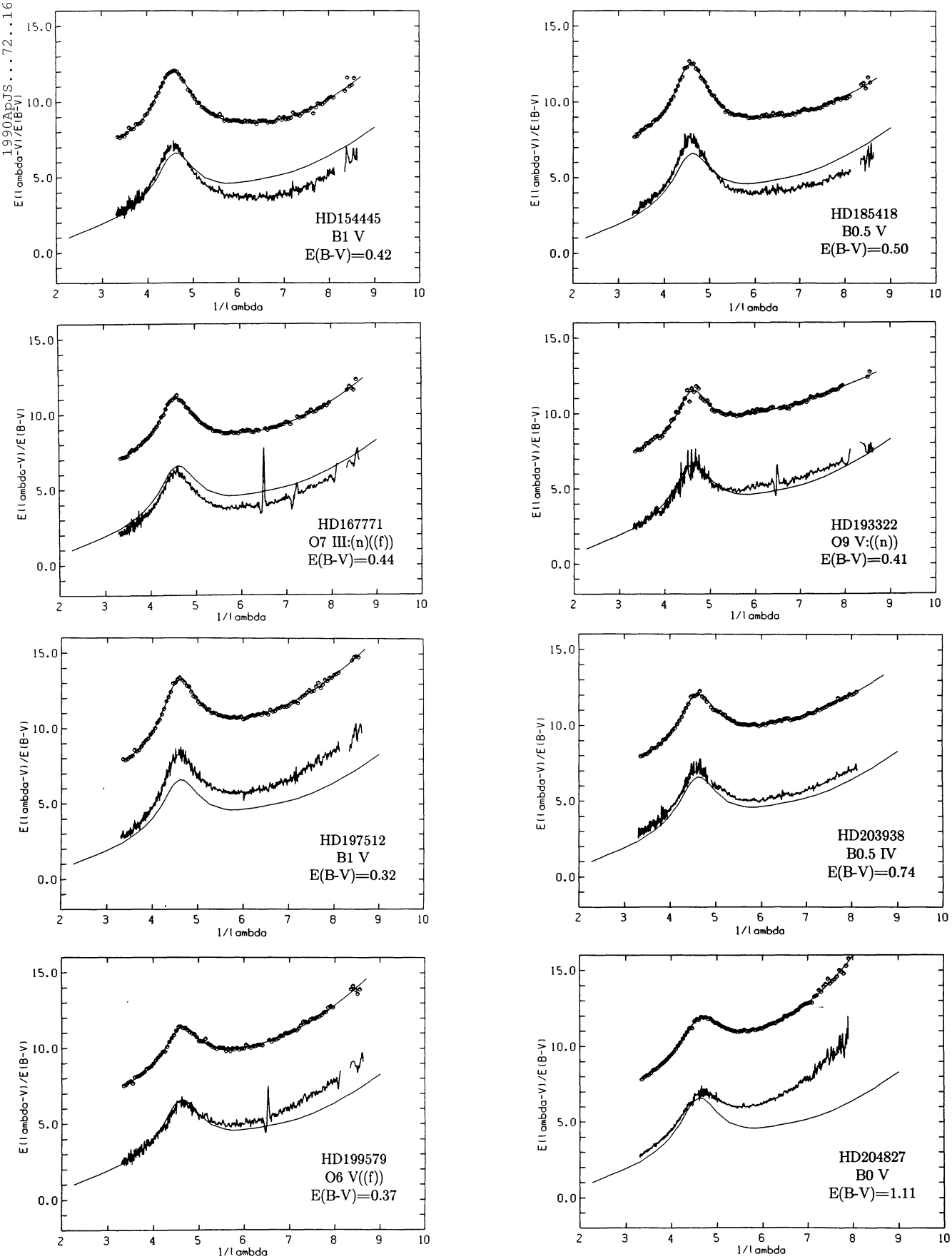

FIG. 2—*Continued*

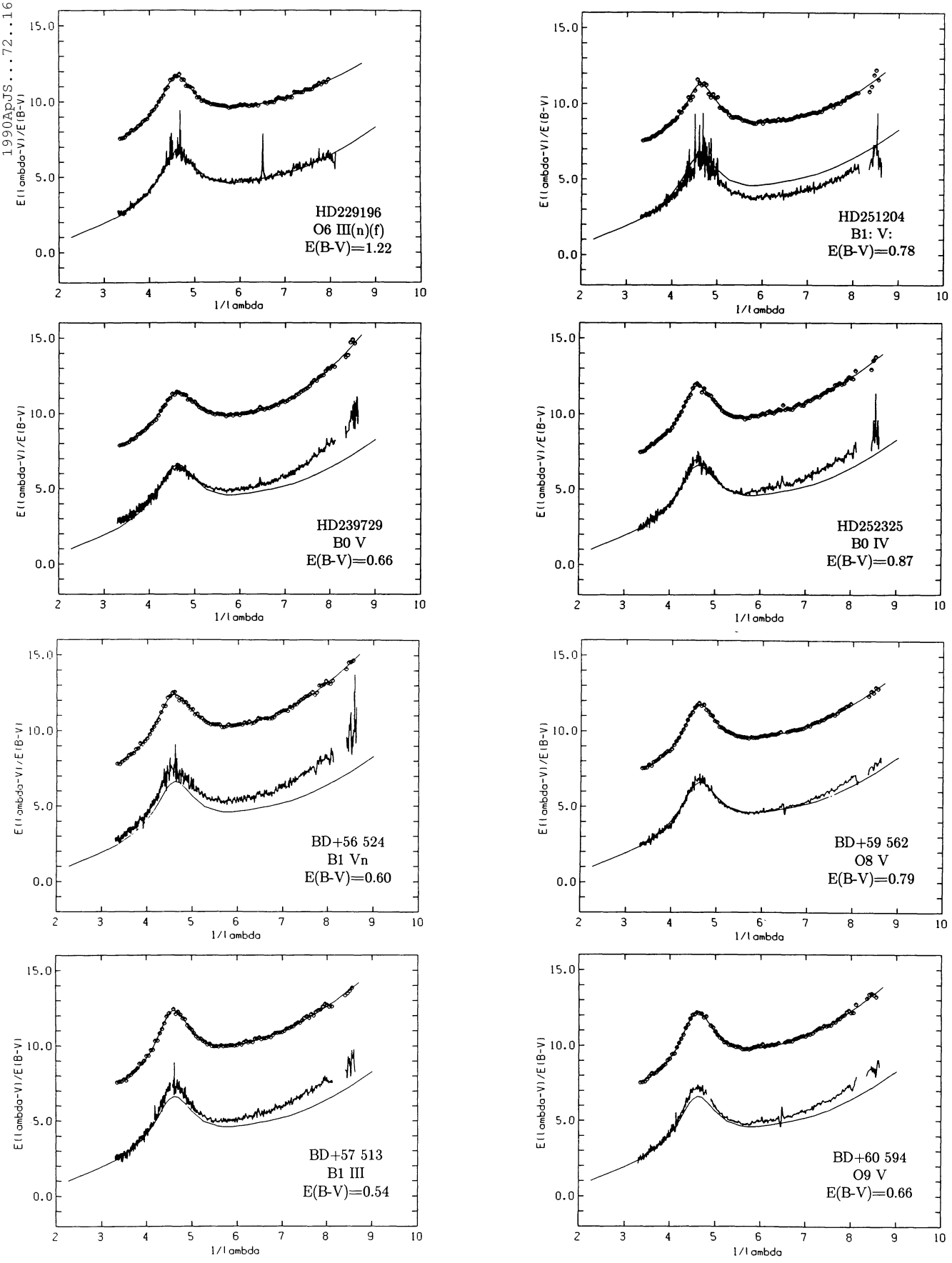

FIG. 2—*Continued*

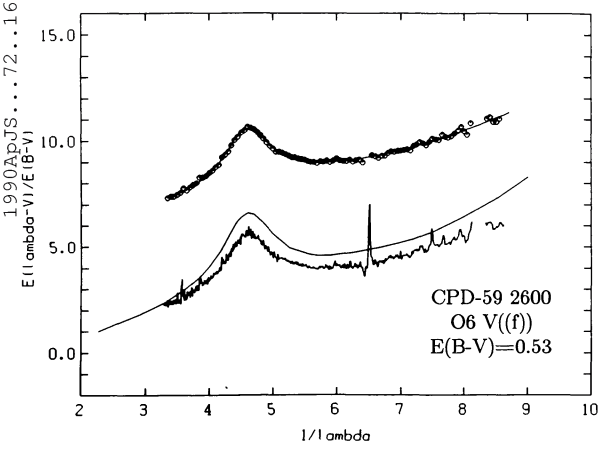

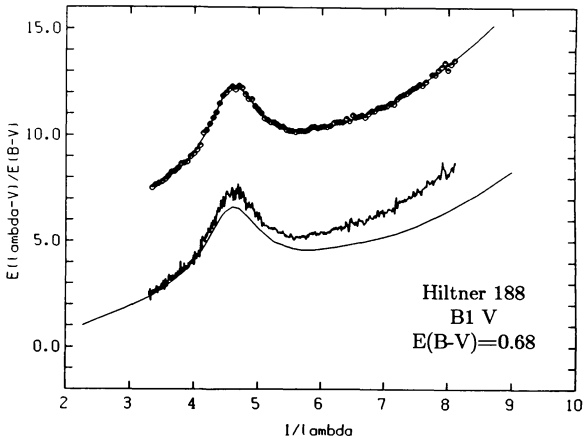

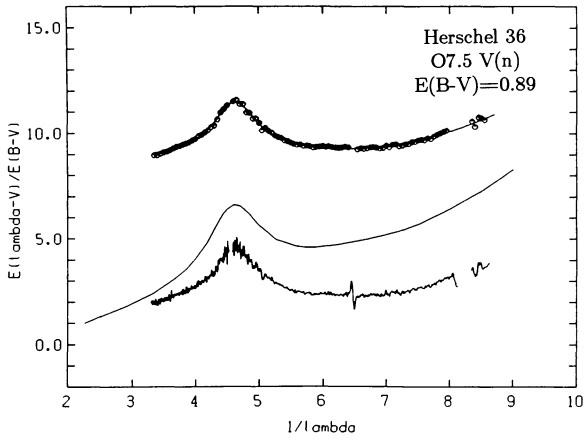

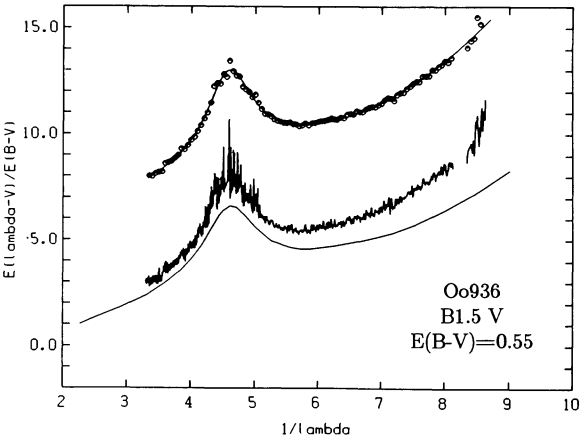

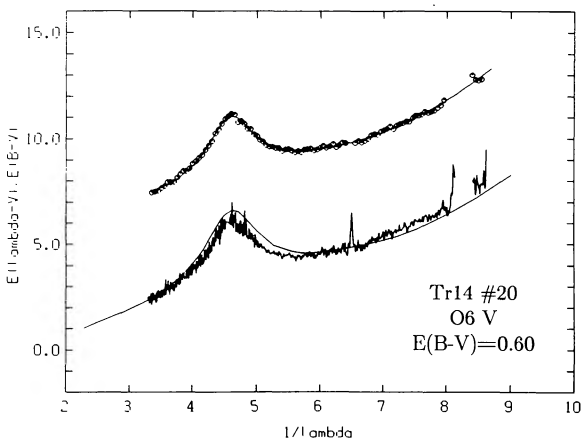

FIG. 2—*Continued*

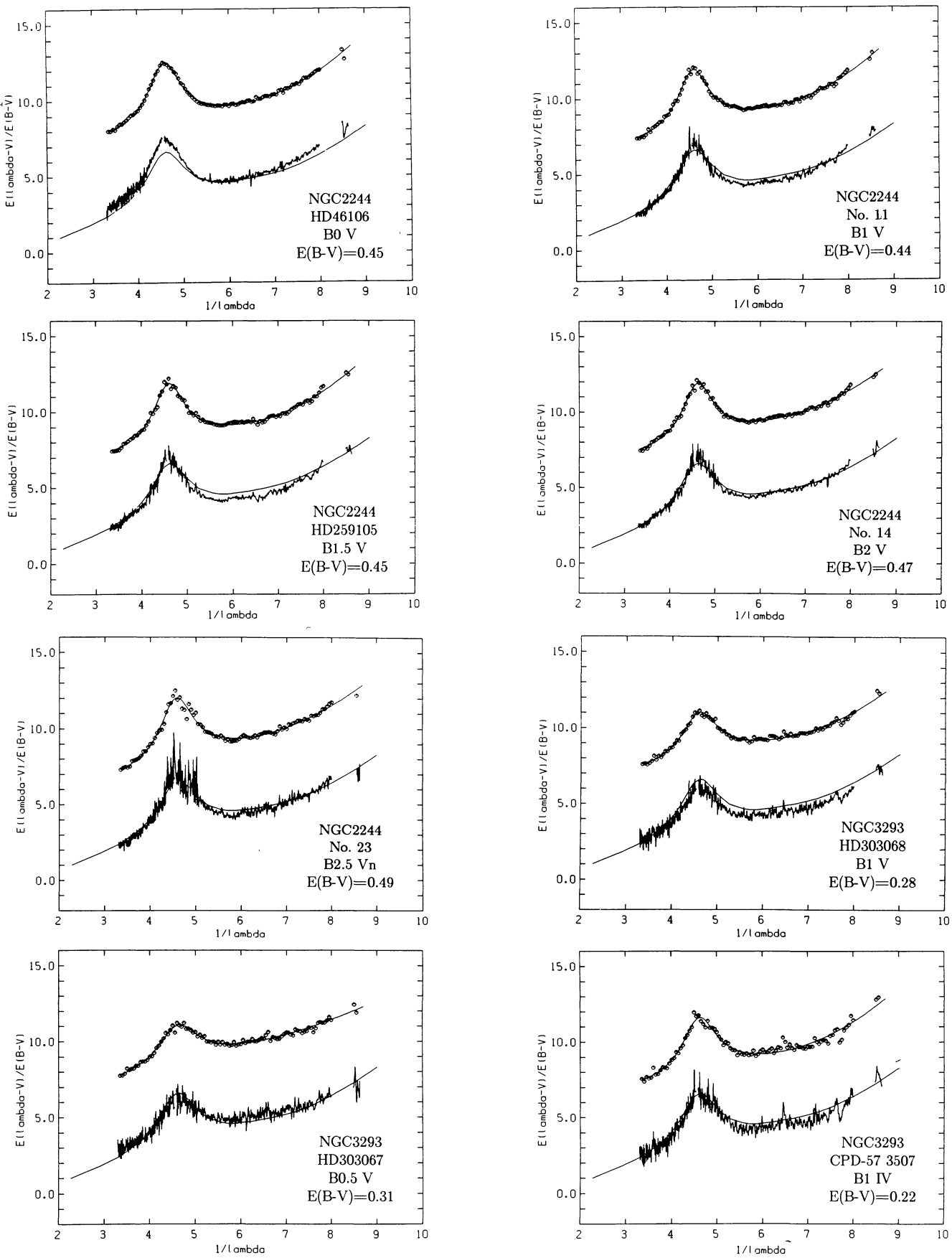

FIG. 3.—Same as Fig. 2 for the cluster stars

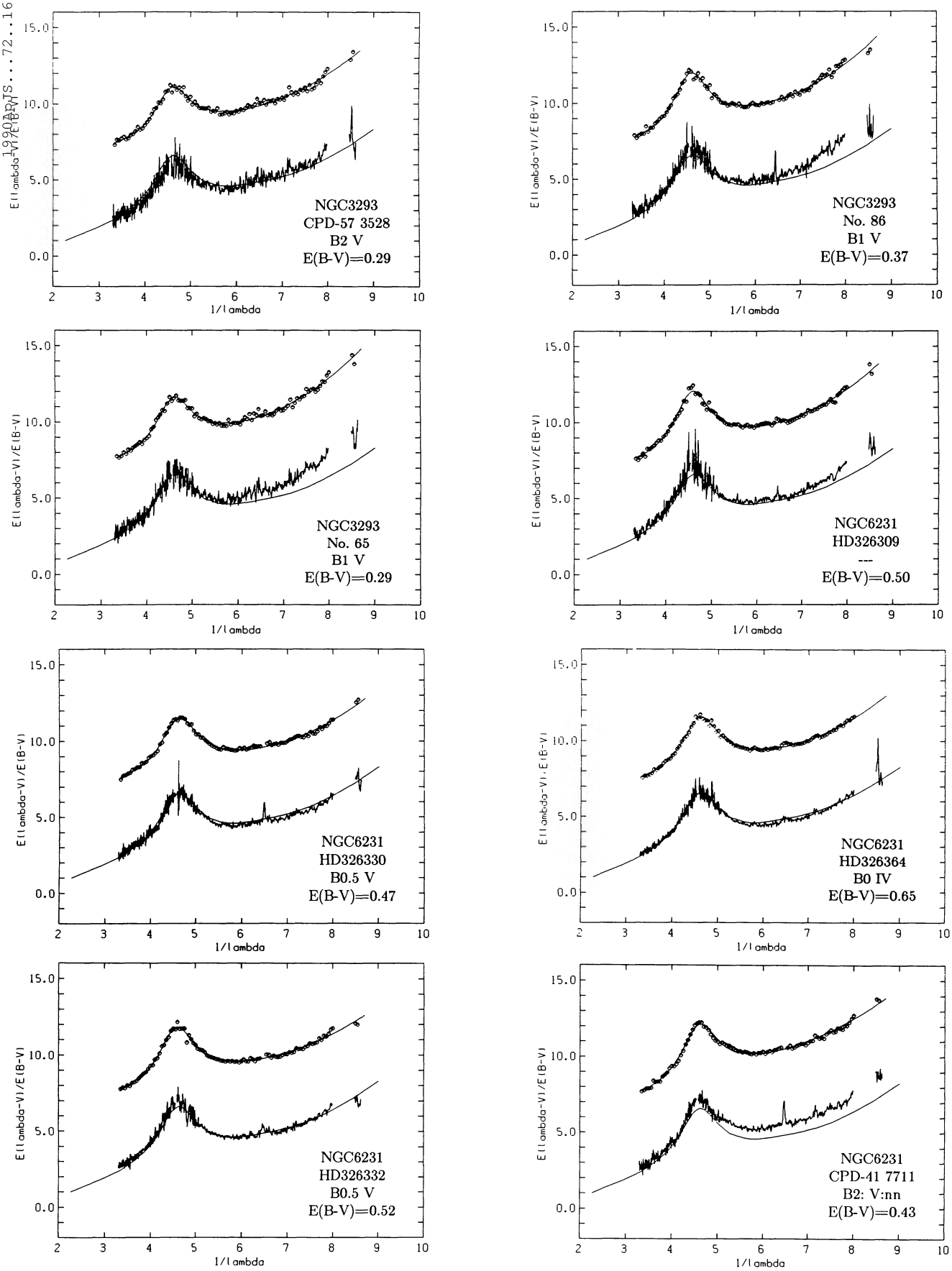

FIG. 3—*Continued*

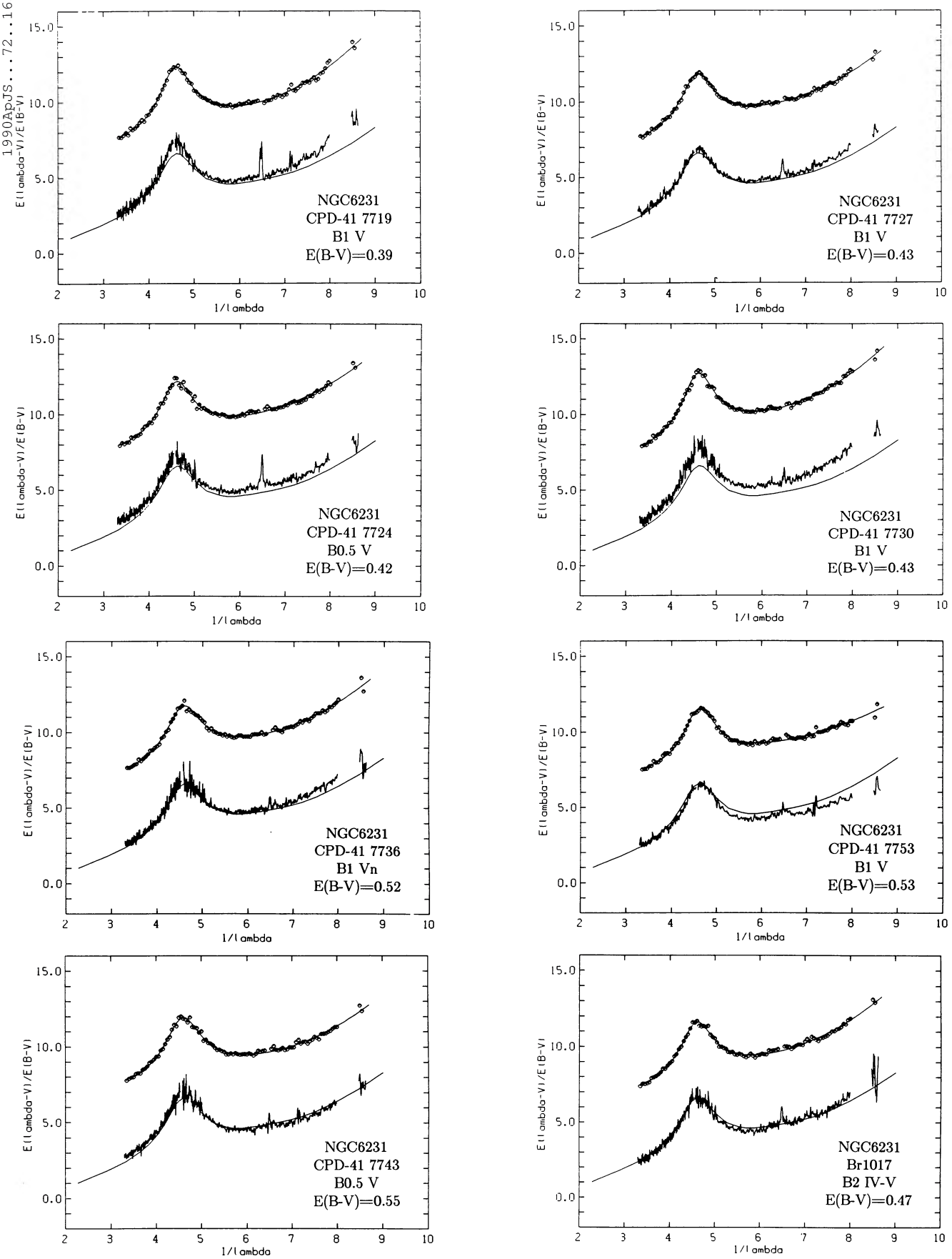

FIG. 3—*Continued*

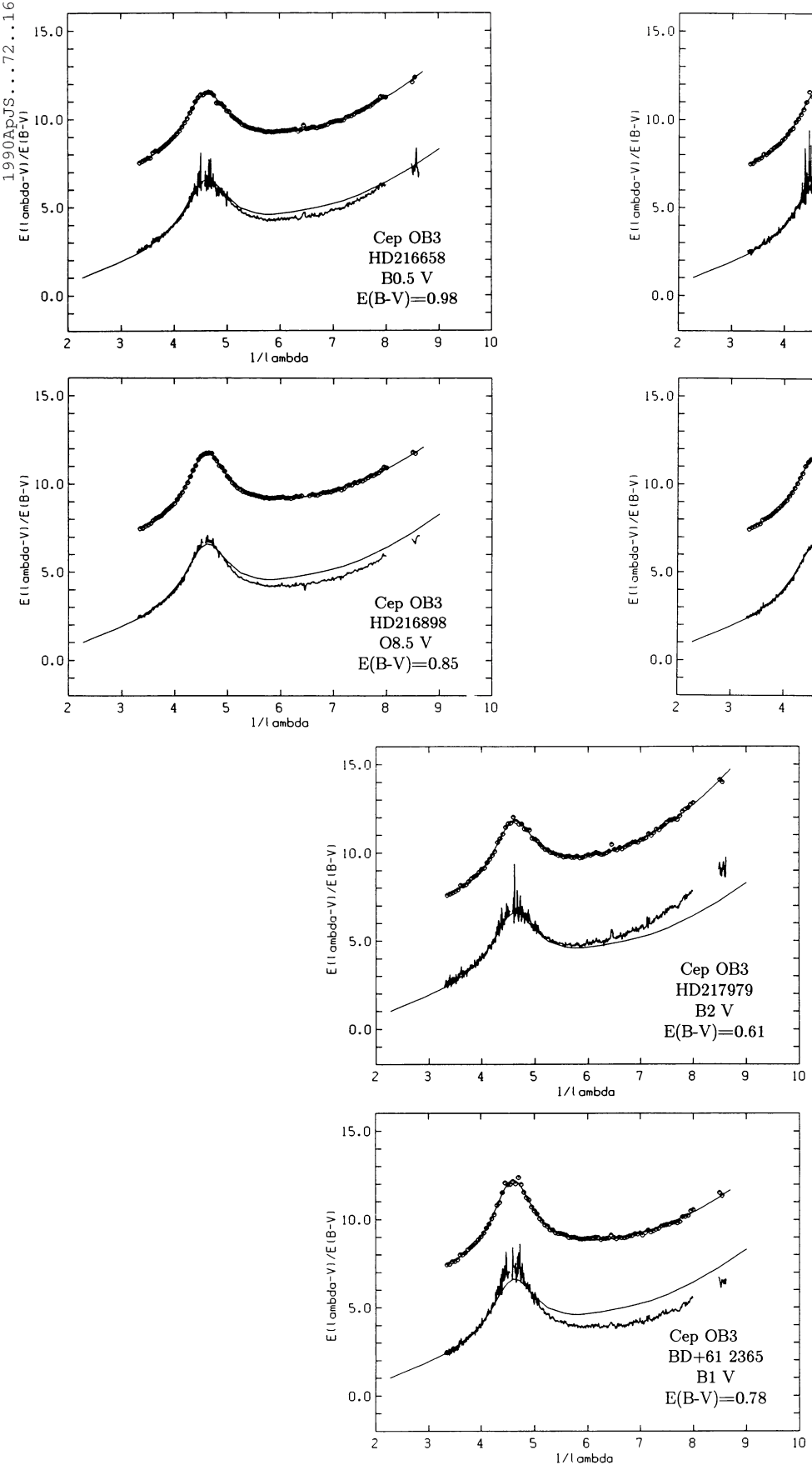

FIG. 3—*Continued*

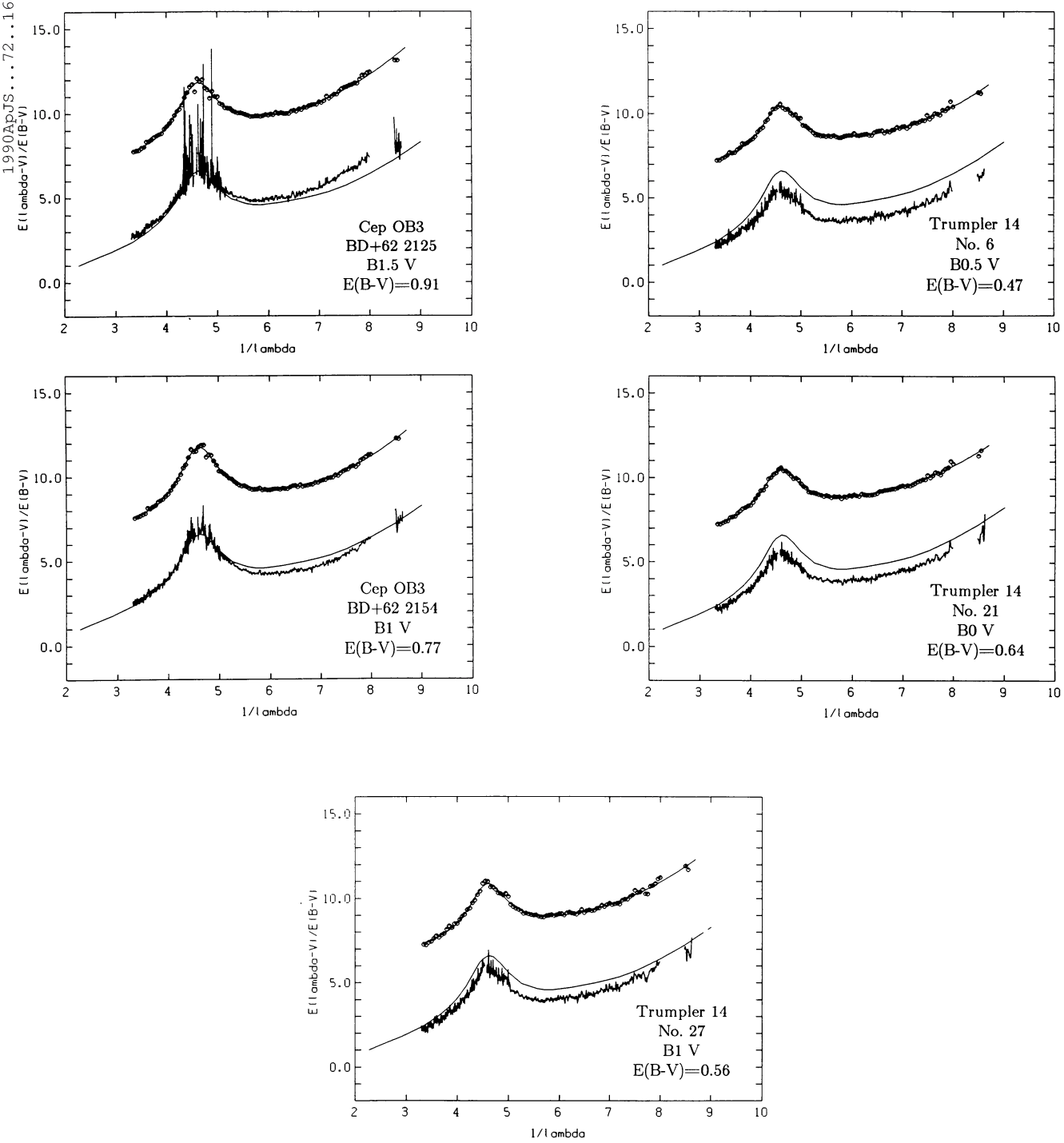

FIG. 3—*Continued*

because the mean of the log is not the same as the log of the mean.

Finally, the binned flux ratio curves are converted to magnitudes and normalized by $(B-V)-(B-V)_{\rm STD}$.

d) *Estimation of the Parameters*

Each extinction curve was fitted by equation (2) using a nonlinear least squares grid search routine. This routine is a straightforward modification of one given by Bevington (1969) and is reproduced in the Appendix for the sake of completeness. The curves were fitted over the region 3.3–8.7 $\mu{\rm m}^{-1}$, with the interval surrounding the 2175 Å bump, 3.3–5.9 $\mu{\rm m}^{-1}$, given twice the weight of the rest of the curve. This weighting was adopted because the far-UV is susceptible to small mismatch errors. Therefore, to keep the far-UV from corrupting our estimates of the bump parameters, we halved its weight. This weighting scheme gives bump parameters which agree with those found by fitting only the bump region and does not degrade the far-UV fits.

Values of the fit parameters are given in Table 5. The first two columns list the program stars and the flux standards used to produce their extinction curves. Values of $E(B-V)$ and $E(B-V)/d$ are given in columns (3) and (4), where the latter quantities are frequently useful for making physical interpretations (Spitzer 1985). The fit parameters are listed in columns (5)–(10). Table 6 gives similar data for the cluster stars. Columns (1) and (2) give the star and flux standard used to produce the curve, column (3) lists the color excess, and the fit parameters are listed in columns (4)–(9). Recall that the shape of the UV extinction toward Cep OB 3 is known to be variable (Massa and Savage 1984).

e) *Determination of the Errors*

Pair method curves are affected by both random and systematic errors. Massa, Savage, and Fitzpatrick (1983) describe these errors and discuss how to estimate their effects. Mismatch of the intrinsic colors of the program and comparison stars is by far the largest single contribution to the overall error budget in most instances. Although it is a straightforward process to evaluate the effect of this contribution on parameters, such as the level of the extinction between 5.5 and 8 $\mu{\rm m}^{-1}$, it is difficult to determine its effect on more complicated measurements of the curve shapes, such as the fit parameters derived from equation (2).

In order to determine the errors in the fitting parameters, it was necessary to return to the extinction data for the cluster stars analyzed by Massa and Fitzpatrick (1986) to establish empirically the magnitude of the errors affecting the parameters. This is accomplished by a two-step process. First, we analyzed the variability of specific curve parameters for several stars in each of the open clusters. These parameters, whose expected errors can be predicted from an error model, are then used to determine whether the extinction curves for all the stars in a given cluster have the same shape, at least as defined by these parameters. If so, then the intracluster scatters in parameters whose errors cannot be accurately predicted *a priori* are taken to represent the observational errors for these parameters. The data in Table 6 (excluding Cep OB 3) were reanalyzed in the manner prescribed by Massa and Fitzpatrick (1986), and the resulting error estimates for the fit parameters are listed in Table 7. The errors listed in the table are for curves with $E(B-V)=1.0$ mag. Recall that the errors scale as $1/E(B-V)$. Therefore, the errors in the coefficients derived from a curve with $E(B-V)$ other than 1.0 mag are given by $\sigma=\sigma_0/E(B-V)$, where σ_0 is the appropriate value from Table 7.

V. THE ATLAS

Figure 2 displays the extinction curves for the program stars, while Figure 3 shows those of the cluster stars. The lower portion of each plot shows the unbinned data, along with Seaton's (1979) mean galactic curve as a fiducial. These plots enable the reader to evaluate the overall quality of the data, including narrow features which may be related to mismatch, and to obtain an impression of how deviant a curve is relative to the galactic mean. Displaced by typically five units above these curves, are the binned data, represented as discrete points, and the analytic fits to these data, shown as solid lines. These curves allow the reader to assess how well the data are represented by equation (2) and the parameters listed in Tables 5 and 6. The star's name, spectral type, and color excess are included on each plot.

We would like to thank the National Space Science Data Center for supplying much of the data used in this paper and M. R. Meade and the MADRAF facility at the University of Wisconsin for help in processing the data. This work was supported by NASA through grants NAS5-29301 to Applied Research Corporation, and NAG5-1014 to Princeton University.

APPENDIX

Table 8 gives the FORTRAN code used to determine the free parameters in equation (2). Implementation of the routine should be self-explanatory through its comment statements.

TABLE 8

CURVE FITTING ROUTINE

```
C ***************************************************************************
C
C
      SUBROUTINE CURVFIT(NPTS,CURV,ALAM,WGHT,WIDTH,CENTROID,
     *                   C1,C2,C3,C4,CHISQR)
C
C       This set of subroutines (CURVFIT, GRIDS, and FITFUNC)
C       performs a simultaneous fit of the near and far UV regions of
C       IUE extinction curves, using the analytical fitting function
C       determined by Fitzpatrick and Massa (1988, Ap.J., May 15).
C       In addition, the subroutine MATINV, found on page 302 of
C       Bevington's (1969) "Data Reduction and Error Analysis for the
C       Physical Sciences" is required.
C
C       The fit is only applicable in the IUE wavelength range, i.e., at
C       wavelengths shortward of about 3000A.  Fitting is initiated by
C       a call to CURVFIT from a user written main program.  The inputs
C       into CURVFIT are the extinction curve values:
C
C               NPTS = number of data points in the curves.
C               ALAM = inverse wavelength (inv. microns) vector.
C               CURV = normalized extinction curve vector.
C               WGHT = data quality vector.  accepts 0's or 1's
C
C       Output from the subroutines consists of:
C
C               WIDTH       = FWHM of the bump (in inv. microns).
C               CENTROID    = location of bump peak.
C               C1,C2,C3,K4 = fitting parameters
C               CHISQR      = chi-squared value of the fit.
C
C ***************************************************************************
C
      REAL*4 CURV(NPTS),ALAM(NPTS),WGHT(NPTS)
      REAL*4 DELT(2)
      REAL*8 BUMP(2),E(4)
      COMMON/BLOCK001/DELT,CHISQ,NPAR,BUMP,E
C
C       Set up some initial parameter values
C
      BUMP(1) = 4.60D0
      BUMP(2) = 1.00D0
      DELT(1) = 0.005
      DELT(2) = 0.005
      CHLAST  = 10.0
C
C       Perform alternating grid searches in bump centroid and width until
C       chi-squared value becomes essentially constant.
C
      DO 200 I = 1,25
          DO 100 NPAR = 1,2
              CALL GRIDS(NPTS,CURV,ALAM,WGHT)
  100     CONTINUE
          DEV = (CHLAST-CHISQ)/((CHLAST+CHISQ)/2.0)
          IF(ABS(DEV) .LT. 0.0001) GO TO 300
          CHLAST = CHISQ
  200 CONTINUE
      WRITE(6,*)' CENTROID & WIDTH UNCONVERGED AFTER 25 ITERATIONS'
  300 CONTINUE
C
C       Recover parameter values to be returned in subroutine call.
C
      CENTROID = BUMP(1)
      WIDTH = SQRT(BUMP(2))
      C1 = E(1)
      C2 = E(2)
```

```
      C3 = E(3)
      C4 = E(4)
      CHISQR = CHISQ
C
C
      RETURN
      END
C
C ***************************************************************************
C
      SUBROUTINE GRIDS(NPTS,CURV,ALAM,WGHT)
C
C     This routine is a modified form of Bevington's GRIDLS routine
C     on pg. 212 of Bevington (1969)
C     A grid search is performed in the parameter BUMP(1) - bump
C     centroid - or in BUMP(2) - bump width.
C
C ***************************************************************************
C
      REAL*4 CURV(NPTS),ALAM(NPTS),WGHT(NPTS),DELT(2)
      REAL*8 BUMP(2),E(4)
      COMMON/BLOCK001/DELT,CHISQ,NPAR,BUMP,E
C
C     Evaluate chi-square at first two search points
C
      DELTA = DELT(NPAR)
      CALL FITFUNC(NPTS,CURV,ALAM,WGHT,CHISQ1)
      FN = 0.0
   50 BUMP(NPAR) = BUMP(NPAR) + DELTA
      CALL FITFUNC(NPTS,CURV,ALAM,WGHT,CHISQ2)
      IF(CHISQ1-CHISQ2) 60,50,70
C
C     Reverse direction of search if chi-squared is increasing
C
   60 DELTA = -DELTA
      BUMP(NPAR) = BUMP(NPAR) + DELTA
      SVE = CHISQ1
      CHISQ1 = CHISQ2
      CHISQ2 = SVE
C
C     Increment parameter until chi-square increases
C
   70 FN = FN + 1.0
      BUMP(NPAR) = BUMP(NPAR) + DELTA
      CALL FITFUNC(NPTS,CURV,ALAM,WGHT,CHISQ3)
      IF(CHISQ3-CHISQ2) 75,100,100
   75 CHISQ1 = CHISQ2
      CHISQ2 = CHISQ3
      GO TO 70
C
C     Find minimum of parabola defined by last 3 points
C
  100 CONTINUE
      DELTA = DELTA*((CHISQ3-CHISQ2)/(CHISQ3-2.0*CHISQ2+CHISQ1)+0.5)
      BUMP(NPAR) = BUMP(NPAR) - DELTA
      DELT(NPAR) = DELT(NPAR)*FN/3.0
C
C     Evaluate function at final parameter value
C
      CALL FITFUNC(NPTS,CURV,ALAM,WGHT,CHISQ)
C
C
      RETURN
      END
C
C ***************************************************************************
```

```
C
      SUBROUTINE FITFUNC(NPTS,CURV,ALAM,WGHT,CHI)
C
C *************************************************************************
C
      REAL*4 CURV(NPTS),ALAM(NPTS),WGHT(NPTS),DELT(2)
      REAL*8 BUMP(2),E(4)
      REAL*8 C(10,10),D(4),WW,XX,YY,XL,XF
      REAL*8 XBUM,XLIN,XFUV,A1,A2,A3,A4,X
      COMMON/BLOCK001/DELT,CHISQ,NPAR,BUMP,E
C
      XLIN(A1,A2,X) = A1 + A2*X
      XBUM(A3,X) = A3/((X-BUMP(1)*BUMP(1)/X)**2.0D0 + BUMP(2))
      XFUV(A4,X) = A4 * (0.53920D0*(X-5.9D0)*(X-5.9D0) +
     *                   0.05644D0*(X-5.9D0)*(X-5.9D0)*(X-5.9D0))
C
C     Zero out needed areas of arrays
C
      DO 50 I = 1,4
          E(I) = 0.0D0
          D(I) = 0.0D0
          DO 25 J = 1,4
              C(I,J) = 0.0D0
   25     CONTINUE
   50 CONTINUE
C
C     Calculate elements of least-squares matrix.  Bump
C     region is given twice the weight of the FUV region.
C
      NPL = 0
      DO 100 I = 1,NPTS
              WW = 1.0D0
              IF(ALAM(I) .LT. 5.9) WW = 2.0D0
              IF(ALAM(I) .LT. 3.3) GO TO 100
              IF(WGHT(I) .EQ. 0.0) GO TO 100
              NPL = NPL + (1*WW+0.5)
              XX = ALAM(I)
              YY = CURV(I)
              XL = XBUM(1.0D0,XX)
              XF = XFUV(1.0D0,XX)
              IF(XX.LT.5.9) XF = 0.0D0
C
              C(1,2) = C(1,2) + XX*WW
              C(1,4) = C(1,4) + XF*WW
              C(2,2) = C(2,2) + XX*XX*WW
              C(2,4) = C(2,4) + XX*XF*WW
              C(3,1) = C(3,1) + XL*WW
              C(3,2) = C(3,2) + XX*XL*WW
              C(3,3) = C(3,3) + XL*XL*WW
              C(3,4) = C(3,4) + XL*XF*WW
              C(4,4) = C(4,4) + XF*XF*WW
              D(1)   = D(1)   + YY*WW
              D(2)   = D(2)   + YY*XX*WW
              D(3)   = D(3)   + YY*XL*WW
              D(4)   = D(4)   + YY*XF*WW
  100 CONTINUE
C
C     Fill in symmetric elements of matrix
C
              C(1,1) = NPL*1.0D0
              C(1,3) = C(3,1)
              C(2,1) = C(1,2)
              C(2,3) = C(3,2)
              C(4,1) = C(1,4)
              C(4,2) = C(2,4)
              C(4,3) = C(3,4)
```

```
C
C       Invert the matrix
C
        CALL MATINV(C,4,DET)
C
C       Solve for coefficients
C
        DO 205 I = 1,4
        DO 200 J = 1,4
                E(I) = E(I) + C(I,J)*D(J)
  200   CONTINUE
  205   CONTINUE
C
C       Calculate reduced chi-squared for the fit. (Bump still weighted
C       twice.)
C
        CHI = 0.0
        DO 300 I = 1,NPTS
                WG = 1.0
                IF(ALAM(I) .LT. 5.9) WG = 2.0
                IF(ALAM(I) .LT. 3.3) GO TO 300
                IF(WGHT(I) .EQ. 0.0) GO TO 300
                XX = ALAM(I)
                XF = XFUV(E(4),XX)
                IF(XX .LT. 5.9) XF = 0.0
                YVAL = XLIN(E(1),E(2),XX) + XBUM(E(3),XX) + XF
                CHI  = CHI + (YVAL-CURV(I))*(YVAL-CURV(I))*WG
  300   CONTINUE
        CHI = CHI/(1.0*(NPL-6))
C
C
        RETURN
        END
```

REFERENCES

Aiello, S., Garesllа, B., Chlewicki, G., Greenberg, J. M., Patriaichi, P., and Perinotto, M. 1988, *Astr. Ap. Suppl.*, **73**, 323.
Bertiau, F. C. 1958, *Ap. J.*, **128**, 533.
Bevington, P. R. 1969, *Data Reduction and Error Analysis for the Physical Sciences* (New York: McGraw-Hill).
Blaauw, A. 1956, *Ap. J.*, **123**, 408.
Blanco, V. M., Demers, S., Douglass, G. G., and FitzGerald, M. P. 1968, *Pub. US Naval Obs.*, **21**, 1.
Boggess, A., *et al.* 1978*a*, *Nature*, **275**, 372.
_____. 1978*b*, *Nature*, **275**, 377.
Bohlin, R. C. 1975, *Ap. J.*, **200**, 402.
Bohlin, R. C., and Grillmair, C. J. 1988, in *IUE NASA Newsletter*, No. 35, p. 161.
Bohlin, R. C., and Holm, A. V. 1980, in *IUE NASA Newsletter*, No. 10, p. 37.
Bohlin, R. C., Savage, B. D., and Drake, J. F. 1978, *Ap. J.*, **224**, 132.
Bohren, C. F., and Huffmann, D. R. 1983, *Absorption and Scattering of Light by Small Particles* (New York: Wiley-Interscience).
Bok, B. J., Bok, P. F., and Graham, J. A. 1966, *M.N.R.A.S.*, **131**, 247.
Braes, L. L. E. 1967, *Bull. Astr. Inst. Netherlands Suppl.*, **2**, 1.
Cardelli, J. A., Clayton, G. C., and Mathis, J. S. 1988, *Ap. J. (Letters)*, **329**, L33.
Carnochan, D. J. 1986, *M.N.R.A.S.*, **219**, 903.
Cousins, A. W. J. 1964, *M.N.A.S. So. Africa*, **32**, 175.
Cousins, A. W. J., and Stoy, R. H. 1962, *Roy. Obs. Bull.*, No. 64.
Crawford, D. L. 1963, *Ap. J.*, **137**, 523.
Crawford, D. L., and Barnes, J. V. 1970, *A.J.*, **75**, 952.
Feinstein, A., Marraco, H. G., and Forte, J. C. 1976, *Astr. Ap. Suppl.*, **24**, 389.
Feinstein, A., Marraco, H. G., and Muzzio, J. C. 1973, *Astr. Ap. Suppl.*, **12**, 331.
FitzGerald, M. P. 1970, *Astr. Ap.*, **4**, 234.
Fitzpatrick, E. L., and Massa, D. 1986, *Ap. J.*, **307**, 286 (Paper I).
_____. 1988, *Ap. J.*, **328**, 734 (Paper II).
Garrison, R. F. 1967, *Ap. J.*, **147**, 1003.
_____. 1970, *A.J.*, **75**, 1001.
Garrison, R. F., and Schild, R. E. 1979, *A.J.*, **84**, 1020.
Guetter, H. H. 1968, *Pub. A.S.P.*, **80**, 197.
_____. 1975, *Pub. A.S.P.*, **86**, 795.
Hardie, R. H., and Crawford, D. L. 1961, *Ap. J.*, **133**, 843.
Hardie, R. H., Heiser, A. M., and Tolbert, C. R. 1964, *Ap. J.*, **140**, 1472.
Hecht, J., Helfer, H. L., Wolf, J., Donn, B., and Pipher, J. L. 1983, *Ap. J. (Letters)*, **263**, L39.
Heiser, A. M. 1977, *A.J.*, **82**, 973.
Hiltner, W. A. 1956, *Ap. J. Suppl.*, **2**, 389.
Hiltner, W. A., Garrison, R. F., and Schild, R. E. 1969, *Ap. J.*, **157**, 313.
Hiltner, W. A., and Johnson, H. L. 1956, *Ap. J.*, **124**, 367.
Hoffleit, D. 1982, *The Bright Star Catalog* (Yale University Obs.).
Holm, A. V., and Schiffer, F. H. 1980, in *IUE NASA Newsletter*, No. 8, p. 45.
Houck, T. E. 1956, Ph.D. thesis, University of Wisconsin.
Jackson, J. D. 1962, in *Classical Electrodynamics* (New York: Wiley).
Jenkins, E. B., Savage, B. D., and Spitzer, L. 1986, *Ap. J.*, **301**, 355.
Johnson, H. L. 1955, *Ann. d'Ap.*, **18**, 292.
_____. 1962, *Ap. J.*, **136**, 1135.
_____. 1967, *Ap. J.*, **147**, 912.
Johnson, H. L., and Morgan, W. W. 1953, *Ap. J.*, **117**, 313.
_____. 1955, *Ap. J.*, **122**, 429.
Joseph, C. L., Snow, T. P., Seab, C. G., and Crutcher, R. M. 1986, *Ap. J.*, **309**, 771.
Jura, M. 1980, *Ap. J.*, **235**, 63.
Lesh, J. R. 1968, *Ap. J. Suppl.*, **16**, 371.
Levato, H., and Abt, H. A. 1976, *Pub. A.S.P.*, **88**, 712.
Massa, D. 1987, *A.J.*, **94**, 1675.
Massa, D., and Fitzpatrick, E. L. 1986, *Ap. J. Suppl.*, **60**, 305.
Massa, D., and Savage, B. D. 1984, *Ap. J.*, **279**, 310.
Massa, D., Savage, B. D., and Cassinelli, J. P. 1984, *Ap. J.*, **287**, 814.
Massa, D., Savage, B. D., and Fitzpatrick, E. L. 1983, *Ap. J.*, **266**, 662.
Morgan, W. W., Code, A. D., and Whitford, A. E. 1956, *Ap. J. Suppl.*, **2**, 41.
Morgan, W. W., Hiltner, W. A., Neff, J. S., Garrison, R. F., and Osterbrock, D. E. 1965, *Ap. J.*, **142**, 974.

Nicolet, B. 1978, *Astr. Ap. Suppl.*, **34**, 1.
Oosterhoff, P. Th. 1937, *Leiden Ann.*, **17**, 1.
Panek, R. J. 1983, *Ap. J.*, **270**, 169.
Racine, R. 1968, *A.J.*, **73**, 233.
Savage, B. D. 1975, *Ap. J.*, **199**, 92.
Savage, B. D., Massa, D., Meade, M., and Wesselius, P. R. 1985, *Ap. J. Suppl.*, **59**, 397.
Schild, R. E. 1965, *Ap. J.*, **142**, 979.
Schild, R. E., Hiltner, W. A., and Sanduleak, N. 1969, *Ap. J.*, **156**, 609.
Schild, R. E., Neugebauer, G., and Westphal, J. A. 1971, *A.J.*, **76**, 237.
Seaton, M. J. 1979, *M.N.R.A.S.*, **187**, 73P.
Sharpless, S. 1952, *Ap. J.*, **116**, 251.
Shobbrook, R. R. 1983, *M.N.R.A.S.*, **205**, 1229.
Shull, J. M., and Van Steenberg, M. E. 1985, *Ap. J.*, **294**, 599.
Simonson, S. C. 1968, *Ap. J.*, **154**, 923.
Spitzer, L. 1985, *Ap. J. (Letters)*, **290**, L21.
Turner, D. G., Grieve, G. R., Herbst, W., and Harris, W. E. 1980, *A.J.*, **85**, 1193.
Van Altena, W. F., and Jones, B. J. 1972, *Astr. Ap.*, **20**, 425.
Walborn, N. R. 1971, *Ap. J. Suppl.*, **23**, 257.
_____. 1972, *A.J.*, **77**, 312.
_____. 1973, *A.J.*, **78**, 1067.
_____. 1982, *A.J.*, **87**, 1300.
Wildey, R. L. 1964, *Ap. J. Suppl.*, **8**, 439.
Wu, C.-C., *et al.* 1983, in *IUE NASA Newsletter*, No. 22., p. 1.

EDWARD L. FITZPATRICK: Princeton University Observatory, Peyton Hall, Princeton, NJ 08544.

DERCK MASSA: Applied Research Corporation, 8201 Corporate Drive, Landover, MD 20785